

Supplementary Information

Authors: Alexandra Crowe, Wei Zheng, Jonathan Miller, Sonia Pahwa, Khondoker Alam, Kar-Ming Fung, Erin Rubin, Feng Yin, Kai Ding, and Wei Yue

Title: Characterization of plasma membrane localization and phosphorylation status of organic anion transporting polypeptide (OATP) 1B1 c.521 T>C nonsynonymous single-nucleotide polymorphism

Journal: Pharmaceutical Research

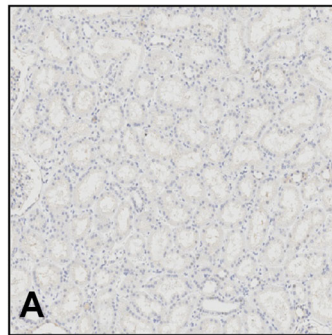
Table S I. Demographics, diagnosis and genotype of c. 521 T>C and c.388 A>G and haplotype of liver donors (*, normal liver tissues as described in the methods)

Subject #	Gender	Age	c.521 T>C	c.388 A>G	Haplotype	Diagnosis
1*	M	21	TC	AG	*1A/*15 or *1B/*5	Gunshot wounds (GSW) benign liver parenchyma
2	F	52	TT	AA	*1A/*1A	Metastatic breast carcinoma
3	F	81	TC	AG	*1A/*15 or *1B/*15	Metastatic colonic adenocarcinoma
4	M	61	TT	GG	*1B/*1B	Metastatic colonic adenocarcinoma
5	F	56	TT	GG	*1B/*1B	Pseudocyst
6	F	61	TT	AA	*1A/*1A	Metastatic colonic adenocarcinoma, Cirrhotic liver
7	M	39	TT	AA	*1A/*1A	Metastatic colonic adenocarcinoma
8	F	72	TT	AA	*1A/*1A	Hepatocellular carcinoma
9*	M	34	TT	AA	*1A/*1A	Steatohepatitis (no fibrosis)
10*	M	65	TT	GG	*1B/*1B	GSW benign liver parenchyma
11	F	75	TT	AG	*1A/*1B	Intrahepatic cholangiocarcinoma
12	F	56	TC	AG	*1A/*15 or *1B/*5	Cavernous hemangioma
13	F	52	TT	GG	*1B/*1B	Hepatocellular carcinoma, Cirrhotic liver
14	M	60	TT	AG	*1A/*1B	Hepatocellular carcinoma, Cirrhotic Liver
15	M	64	TC	AG	*1A/*15 or *1B/*5	Metastatic colonic adenocarcinoma
16	F	68	TC	AA	*1A/*5	Intrahepatic cholangiocarcinoma
17	M	69	TT	AG	*1A/*1B	Intrahepatic cholangiocarcinoma
18	F	48	TC	AG	*1A/*15 or *1B/*5	Intrahepatic cholangiocarcinoma
19	F	37	TT	AG	*1A/*1B	Hepatic adenoma
20	F	49	TT	AG	*1A/*1B	Hepatocellular carcinoma, Cirrhotic Liver
21	F	28	TT	AG	*1A/*1B	Cavernous hemangioma
22*	F	53	TT	GG	*1A/*1A	Hepatic adenoma
23	M	66	TT	AA	*1B/*1B	Intrahepatic cholangiocarcinoma
24	F	53	TC	AG	*1A/*15 or *1B/*5	Metastatic breast carcinoma
25	F	38	TT	AG	*1A/*1B	Hepatobiliary cystadenoma mucinous cystic neoplasm
26	M	57	TT	AA	*1A/*1A	Metastatic neuroendocrine carcinoma
27	F	73	TC	GG	*1B/*15	Metastatic colonic adenocarcinoma
28	F	59	TT	AA	*1A/*1A	Cavernous hemangioma
29	M	81	TC	AA	*1A/*5	Metastatic colonic adenocarcinoma
30*	M	21	TC	AA	*1A/*5	GSW benign liver parenchyma
31*	M	32	TC	GG	*1B/*15	GSW benign liver parenchyma
32	M	62	TT	AA	*1A/*1A	Intrahepatic cholangiocarcinoma
33	M	52	TT	GG	*1B/*1B	Hepatocellular carcinoma, Cirrhotic Liver
34*	M	31	TT	AG	*1A/*1B	GSW benign liver parenchyma with steatosis
35	M	55	TC	GG	*1B/*15	Metastatic colonic adenocarcinoma

36	F	48	TT	GG	*1B/*1B	Metastatic endometroid adenocarcinoma
37*	M	17	TC	AA	*1A/*5	GSW benign liver parenchyma
38	M	60	TT	AA	*1A/*1A	Metastatic colonic adenocarcinoma, Cirrhotic Liver
39	M	61	TT	AG	*1a/*1b	Cavernous hemangioma
40	F	83	TC	AG	*1A/*15 or *1B/*5	Metastatic colonic adenocarcinoma
41	M	61	CC	AG	*5/*15	Metastatic neuroendocrine carcinoma
42	M	57	TT	AA	*1A/*1A	Hepatocellular carcinoma
43	F	41	TT	AA	*1A/*1A	Chronic hepatitis C
44	F	54	TC	AG	*1A/*15 or *1B/*5	Chronic hepatitis C
45	M	55	TT	AG	*1A/*1B	Chronic hepatitis C
46	M	61	TT	AG	*1A/*1B	Chronic hepatitis C
47	M	55	TT	AA	*1A/*1A	Chronic hepatitis C
48	F	22	TT	AG	*1A/*1B	Chronic hepatitis C
49	M	61	TC	AG	*1A/*15 or *1B/*5	Chronic hepatitis C
50	F	48	TT	AG	*1A/*1B	Chronic hepatitis C
51	M	61	TT	GG	*1B/*1B	Chronic hepatitis C
52	F	54	TT	AA	*1A/*1A	Chronic hepatitis C
53	F	32	TT	GG	*1B/*1B	Chronic hepatitis C
54	M	60	TT	AG	*1A/*1B	Chronic hepatitis C
55	F	63	TT	GG	*1B/*1B	Chronic hepatitis C
56	F	16	TC	GG	*1B/*15	NASH, Diabetes mellitus type 2
57	F	50	TC	GG	*1B/*15	NASH, Diabetes mellitus type 2
58	F	55	CC	AG	*5/*15	Steatohepatitis; borderline diabetes
59	F	41	TC	AA	*1A/*5	Steatohepatitis, Diabetes mellitus type 2
60	M	48	TT	AA	*1A/*1A	Steatohepatitis, Diabetes mellitus type 2, dyslipidemia
61	M	52	TT	AA	*1A/*1A	Steatohepatitis, Diabetes mellitus type 2
62	F	56	TT	AG	*1A/*1B	Steatohepatitis, Diabetes mellitus type 2
63	F	27	TC	AG	*1A/*15 or *1B/*5	NASH, Diabetes mellitus type 2
64	F	41	TT	AG	*1A/*1B	Steatohepatitis, Diabetes mellitus type 2
65	M	50	TC	GG	*1B/*15	Steatohepatitis, Diabetes mellitus type 2, dyslipidemia
66	M	33	TC	AG	*1A/*15 or *1B/*5	Steatohepatitis, Diabetes mellitus type 2
67	F	34	TT	AA	*1A/*1A	Steatohepatitis, Diabetes mellitus type 2, dyslipidemia
68	F	53	TT	AG	*1A/*1B	Steatohepatitis, Diabetes mellitus type 2
69	F	50	TC	GG	*1B/*15	Steatohepatitis, Diabetes mellitus type 2, dyslipidemia
70	M	61	TT	AA	*1A/*1A	Steatohepatitis, hypertension, GERD
71	M	61	TT	GG	*1B/*1B	Steatohepatitis, borderline diabetes, GERD
72	M	21	TT	AA	*1A/*1A	Steatohepatitis, Diabetes mellitus type 1
73	F	65	TT	AG	*1A/*1B	Steatohepatitis, symptomatic cholelithiasis
74	M	42	TT	AG	*1A/*1B	Steatohepatitis, ventral incisional hernia

75	M	47	TT	GG	*1B/*1B	Steatohepatitis, Diabetes mellitus type 2
76	F	52	TT	AG	*1A/*1B	Steatohepatitis, Diabetes mellitus type 2, dyslipidemia
77	F	33	TT	AA	*1A/*1A	Steatohepatitis, Diabetes mellitus type 2, dyslipidemia
78	F	63	TT	AG	*1A/*1B	Steatohepatitis, Diabetes mellitus type 2, dyslipidemia
79	M	48	TT	AG	*1A/*1B	Steatohepatitis, Diabetes mellitus type 2, dyslipidemia

Kidney/OATP1B1



Kidney/OATP1B3

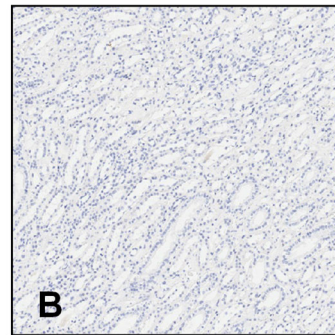


Fig. S I IHC of OATP1B1 and OATP1B3 in human kidney tissues. IHC of OATP1B1 (A) and OATP1B3 (B) (1:1000 dilution) in negative control kidney tissues.

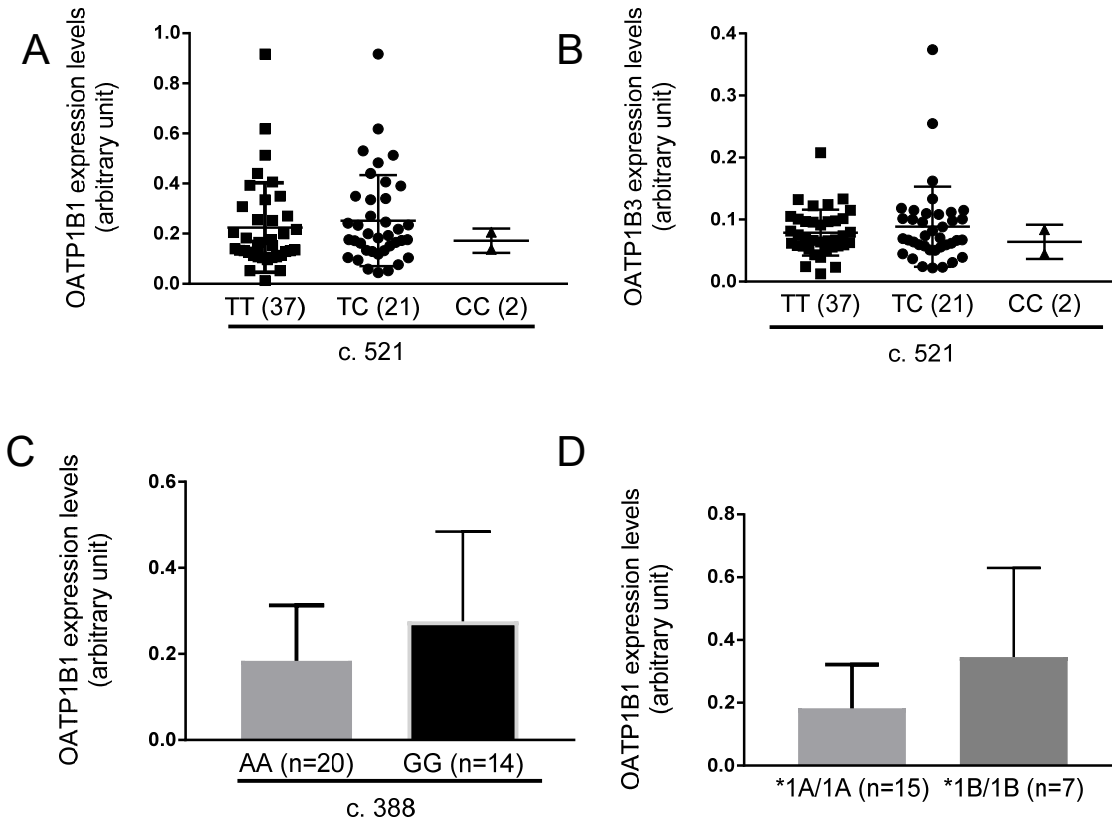


Fig. S II Semi-quantification of OATP1B1 and OATP1B3 IHC in human liver tissue. Semi-quantification of OATP1B1 (A) and OATP1B3 (B) antibody staining in human liver tissue donors genotyped for OATP1B1 c. 521 TT (square, n=37), TC (circle, n=21) and CC (triangle, n=2). Semi-quantification of OATP1B1 expression in human liver tissue donors harboring (C) OATP1B1 c. 388 AA (n=20) and GG (n=14) and (D) *1A/1A (c.388A-c.521T, n=15) and *1B/1B (c.388G-c.521T, n=7). Two-tailed student t-test were conducted in (C) and (D). Non-cirrhotic and non-HCV liver tissues were used in A-D.

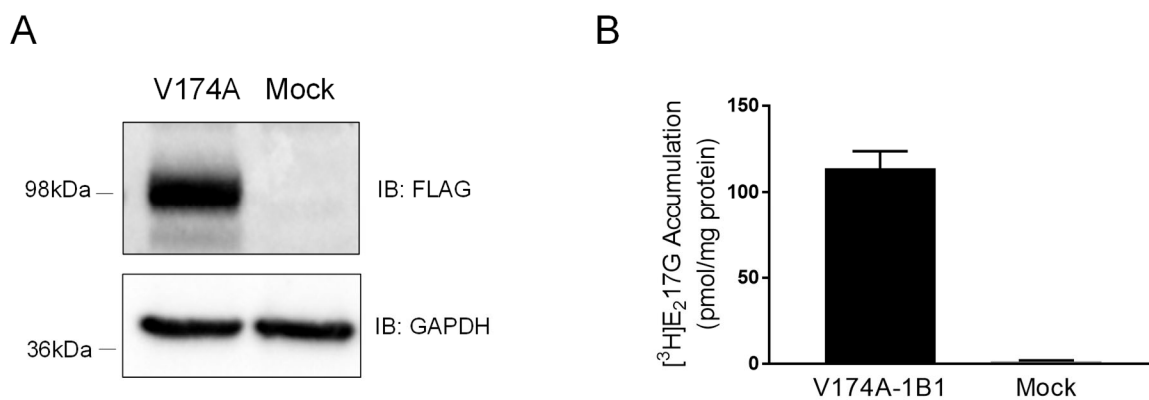


Fig. S III Characterization of HEK293-FLAG-V174A-OATP1B1 stable cell line. (A) Immunoblot of HEK293-FLAG-V174A-OATP1B1 and negative control cell line, HEK293-Mock. Whole cell lysates (50 μg) were separated on a 10% SDS-PAGE gel and probed with FLAG and GAPDH antibodies. FLAG antibody was used to detect OATP1B1 expression. GAPDH served as the loading control. A representative image is shown (n=3). (B) $[^3\text{H}]E_217\beta\text{G}$ (1 μM , 2 min) accumulation of HEK293-FLAG-V174A-OATP1B1 vs. the HEK293-Mock negative control cell line. Data represent mean \pm SD, n=1 (>3 samples).

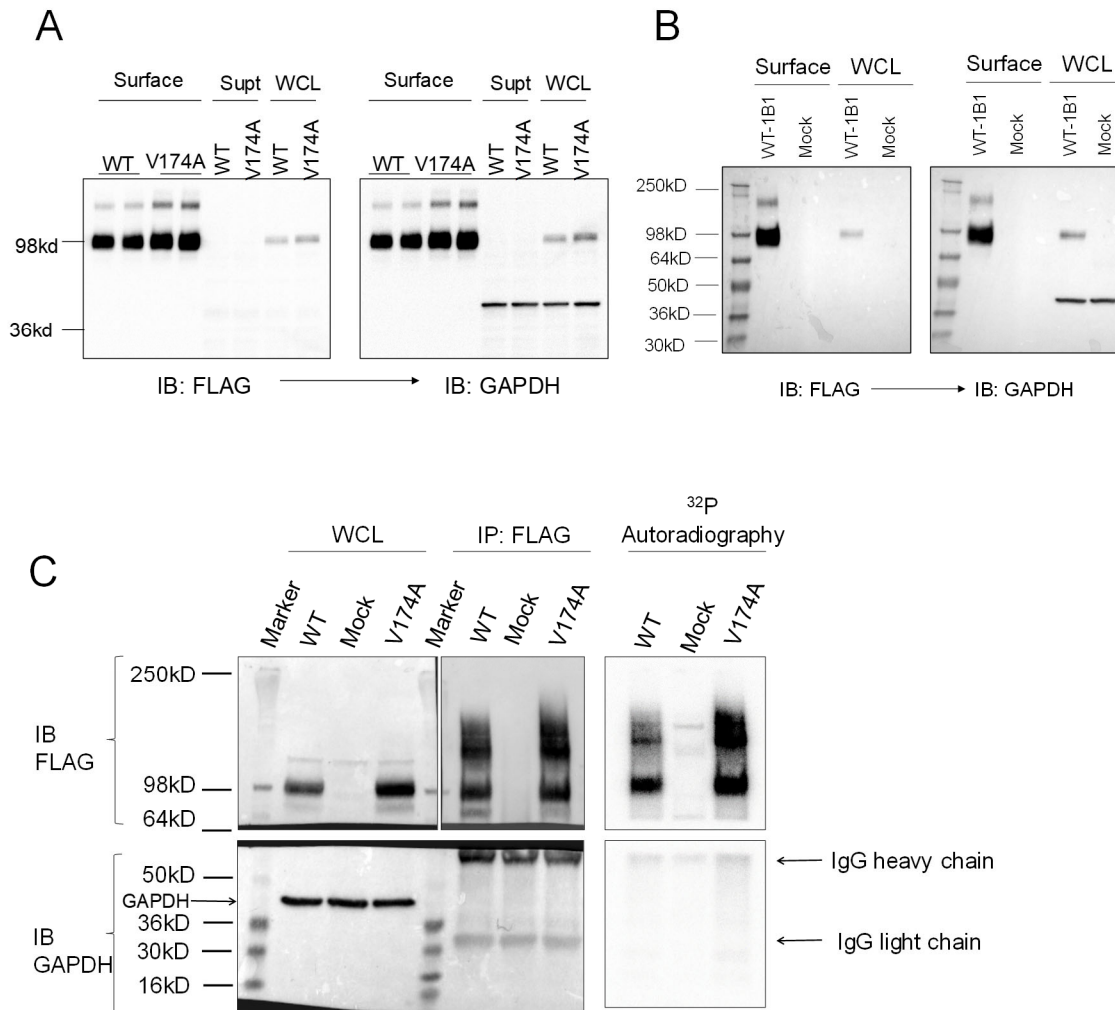


Fig. S IV Full blots of surface biotinylation and phosphorylation determination. (A) Full blots of Fig. III. WT- and V174A-OATP1B1 was determined by pulling down surface proteins with NeutrAvidin beads. From the same blot, the membrane is first probed with an anti-FLAG antibody (A), followed by an anti-GAPDH antibody without stripping. (B) Surface biotinylation followed by FLAG immunoblot in HEK293-FLAG-WT-OATP1B1 and negative control HEK293-Mock cells, showing the upper band is specific to FLAG-OATP1B1. (C) Full blot of Fig. VI A. HEK293-FLAG-WT- and -V174A-OATP1B1 was metabolically labeled with ³²P-orthophosphate for 5 h. After labelling, cells were lysed and whole cell lysates (WCL) (500 µg) were immunoprecipitated (IP) with FLAG antibody and subjected to autoradiography and subsequent immunoblot (IB) with FLAG and GAPDH antibodies. HEK293-Mock cells were used as negative control. Blot was cut at ~64 kD. The upper part was probed with mouse FLAG antibody, and the lower part was probed with mouse GAPDH. Goat anti-mouse secondary antibody was used in immunoblot. After incubation with goat anti-mouse secondary antibody, images were captured.

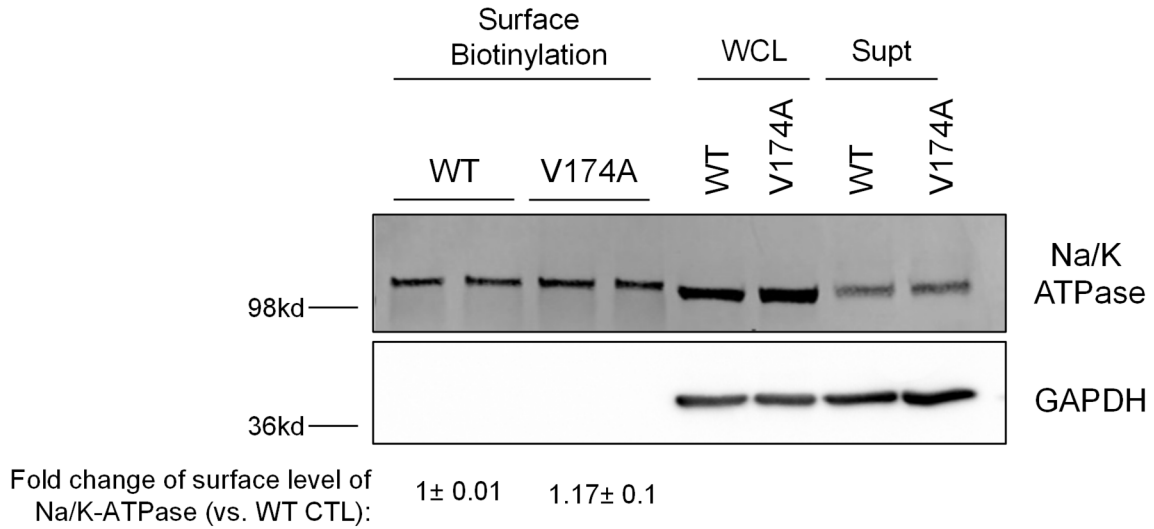


Fig. S V Surface expression of the Na/K-ATPase in HEK293-WT- and -V174A-OATP1B1 cells. Protein levels of Na/K-ATPase in the biotinylated membrane fraction, whole cell lysate (WCL) and intracellular supernatant (Supt). A Na/K-ATPase antibody was used to detect Na/K-ATPase expression and GAPDH was used a cytoplasmic marker. The densitometry of Na/K-ATPase was determined in all fractions. The fold change in the percentage of Na/K-ATPase expressed on the surface was expressed as the amount in the surface fraction divided by the sum of the surface fraction and scaled up supernatant fraction in HEK293-V174A-OATP1B1 vs. HEK293-WT-OATP1B1 (n=1 in duplicate, data represent mean \pm range).

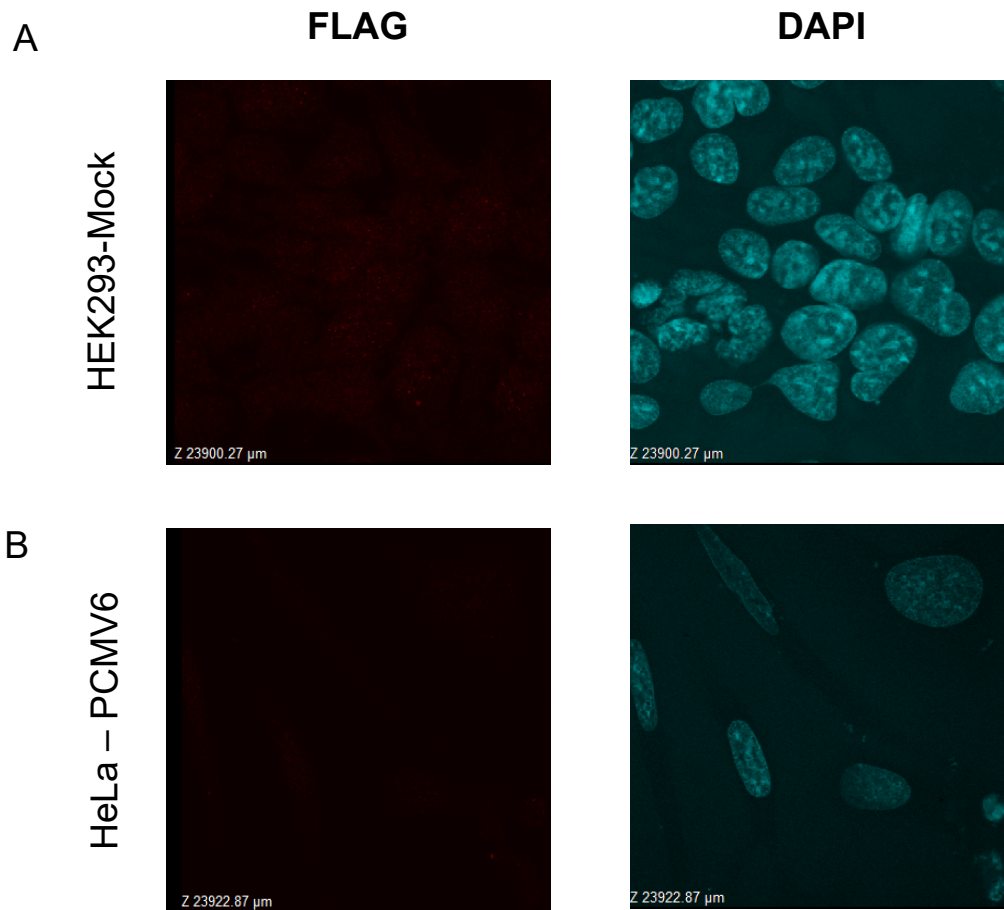


Fig. S VI Immunocytochemistry staining in negative controls. (A) HEK293-Mock stable cell line stained with FLAG antibody. Cells were seeded on coverslips at 1.5×10^5 cells/well and were grown to confluence for 48 h. Cells were stained with FLAG antibody (red) and counterstained with DAPI (blue) to visualize OATP1B1 and nuclei, respectively. (B) HeLa cells transiently transfected and stained with FLAG antibody. HeLa cells were plated on coverslips at a density of 2.5×10^4 cells/well and were transfected with PCMV6 empty vector 24 h later. Forty-eight hours post-transfection, cells were stained with FLAG antibody (red) to visualize OATP1B1 and were counterstained with DAPI (blue) to show nuclei. Images were captured using the Olympus FV10i confocal microscope at a 120X objective and 1024x1024 resolution.

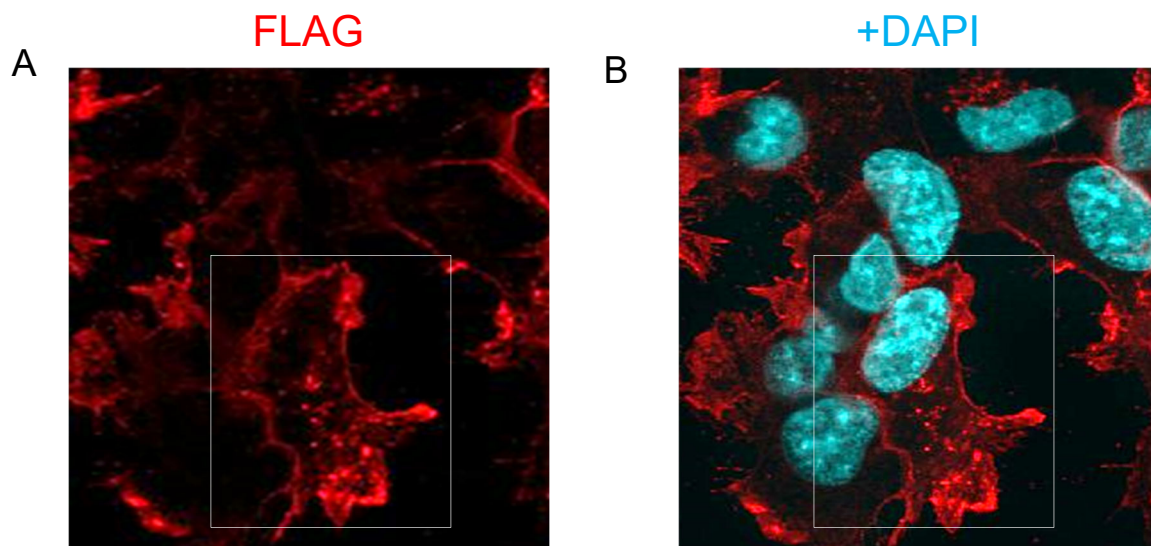


Fig. S VII Amount of intracellular staining of FLAG-OATP1B1 in HEK293-FLAG-WT-OATP1B1 cells. HEK293-FLAG-WT-OATP1B1 cells were seeded at 1.5×10^5 cells/well and grown for 24 h. Cells were fixed and stained with FLAG antibody (1:100, red) (A) and overlaid with DAPI (B) as detailed in the Materials and Methods section.

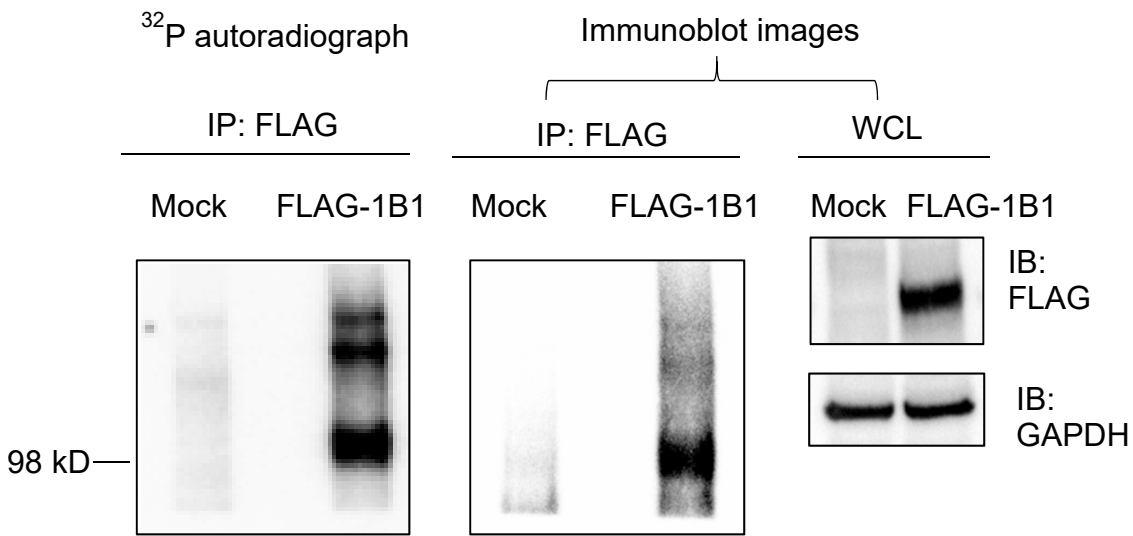


Fig. S VIII Phosphorylation of HEK293-WT-FLAG-OATP1B1. HEK293-FLAG-WT-OATP1B1 stable cell line (2.5×10^6 cells/100mm² dish) was metabolically labelled with ³²P-orthophosphate (0.1mCi/ml) for 5 h at 37°C. (A) HEK293-Mock cells (empty vector) were labelled with ³²P-orthophosphate under the same conditions and were used as a negative control. Lysis, immunoprecipitation (IP), SDS-PAGE, autoradiography, and immunoblot (IB) analyses were performed. ³²P-orthophosphate-labelled FLAG-OATP1B1 in whole cell lysate (WCL) (500 µg) was immunoprecipitated with FLAG antibody. Phosphorylation of OATP1B1 was determined using autoradiography. Immunoblot with FLAG antibody was used to detect FLAG-tagged OATP1B1 expression. GAPDH antibody served as the loading control for WCL.

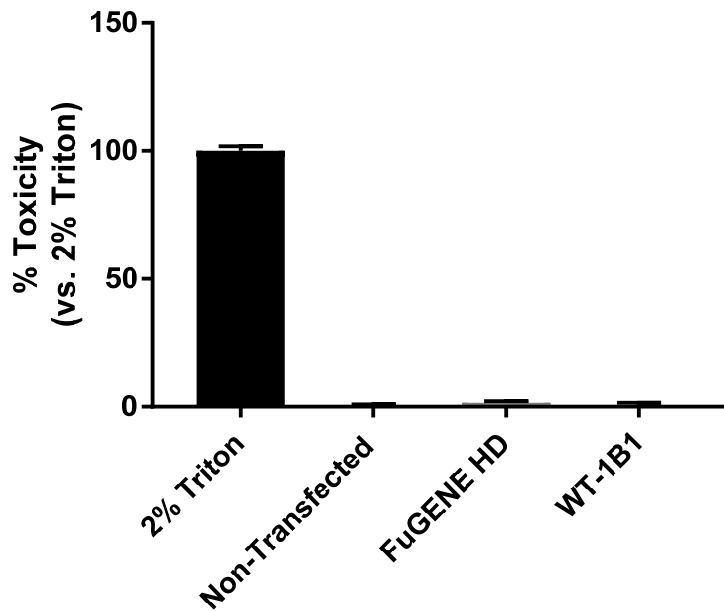
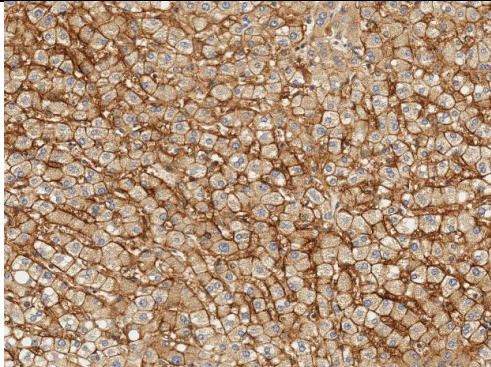
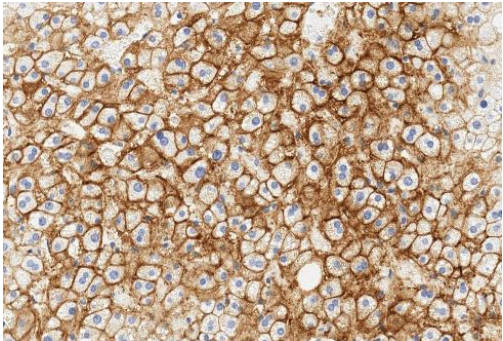
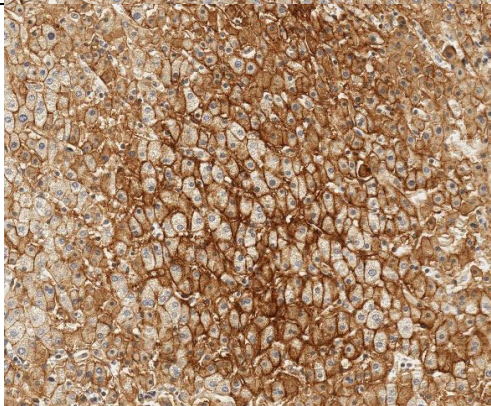
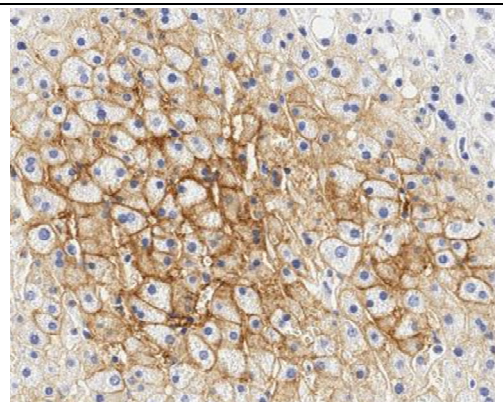

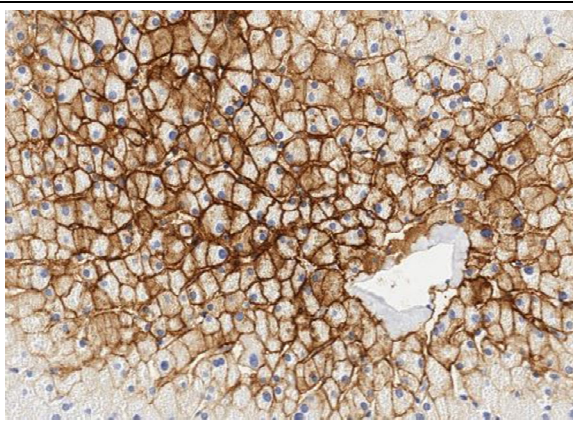
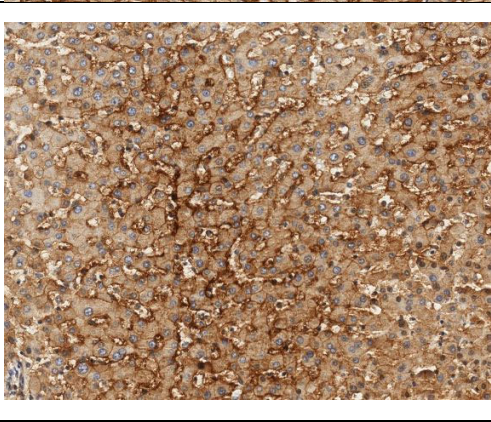
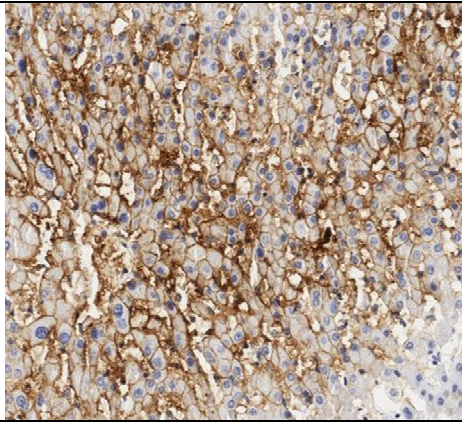
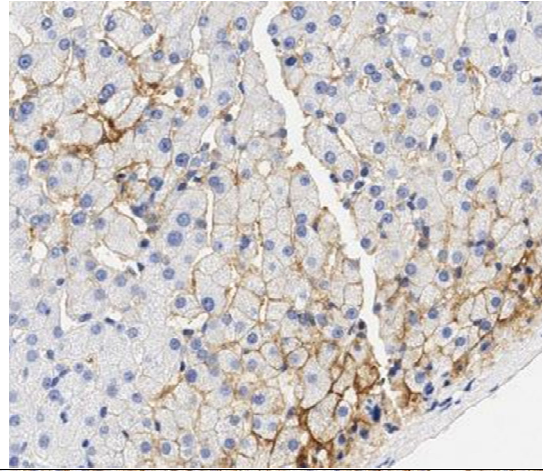
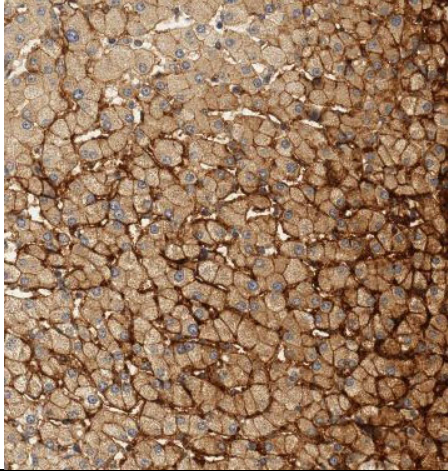


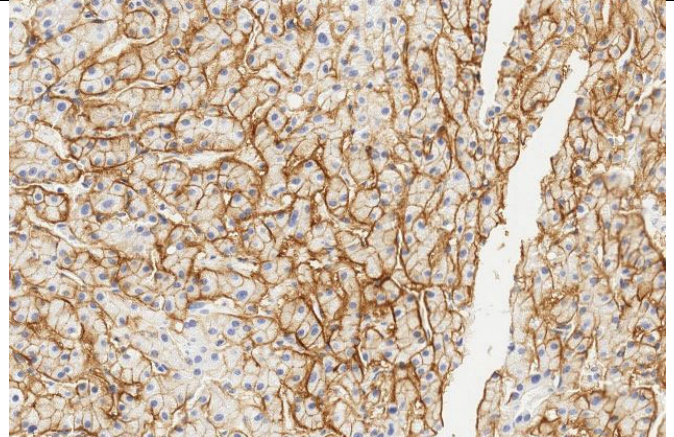
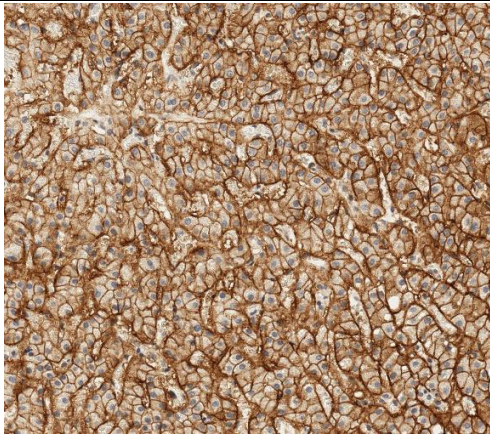
Fig. S IX Lactic Acid Dehydrogenase (LDH) assay testing toxicity of transient transfection in HeLa cells. HeLa cells were seeded at 2.5×10^4 cells/well and transfected with FLAG-WT-OATP1B1, FuGENE HD alone or non-transfected. Forty-eight hours post-transfection, non-transfected cells (in triplicate) were treated with 2% Triton X-100 in DMEM for 30 min at 37°C. Media was collected from all wells and spun down for 2 min at 13,000rpm. Cytotoxicity of non-transfected and transfected cells was determined using the LDH cytotoxicity kit (Sigma, St. Louis, MO), according to manufacturer's instructions. The 2% Triton X-100 treatment served as the positive control ($n=1$ in triplicate).

	IHC: OATP1B1	IHC: OATP1B3
1 NM	 A high-magnification immunohistochemical (IHC) image showing a dense population of cells with brown cytoplasmic staining for OATP1B1. Nuclei are counterstained with blue hematoxylin.	 A high-magnification IHC image showing a dense population of cells with brown cytoplasmic staining for OATP1B3. Nuclei are counterstained with blue hematoxylin.
2	 A high-magnification IHC image showing a dense population of cells with brown cytoplasmic staining for OATP1B1. Nuclei are counterstained with blue hematoxylin.	 A high-magnification IHC image showing a dense population of cells with brown cytoplasmic staining for OATP1B3. Nuclei are counterstained with blue hematoxylin.
3	 A high-magnification IHC image showing a dense population of cells with brown cytoplasmic staining for OATP1B1. Nuclei are counterstained with blue hematoxylin. There is a white artifact in the lower center.	 A high-magnification IHC image showing a dense population of cells with brown cytoplasmic staining for OATP1B3. Nuclei are counterstained with blue hematoxylin. There is a white artifact in the lower center.
4	 A high-magnification IHC image showing a dense population of cells with brown cytoplasmic staining for OATP1B1. Nuclei are counterstained with blue hematoxylin.	 A high-magnification IHC image showing a dense population of cells with brown cytoplasmic staining for OATP1B3. Nuclei are counterstained with blue hematoxylin.

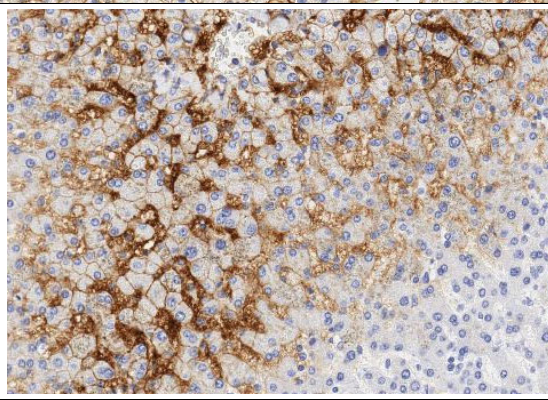
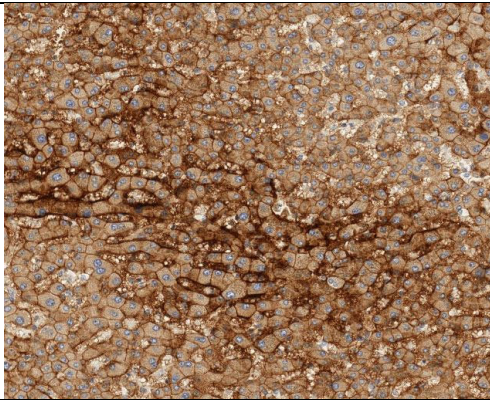
5



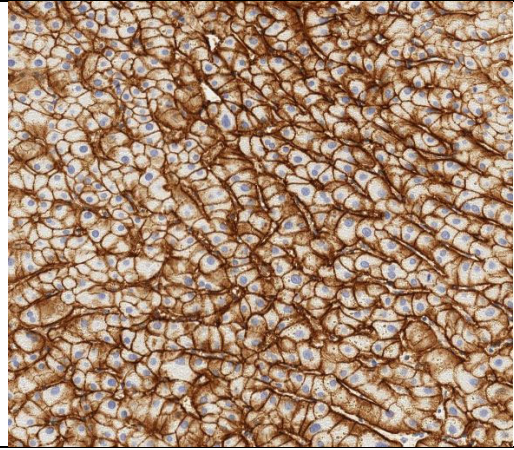
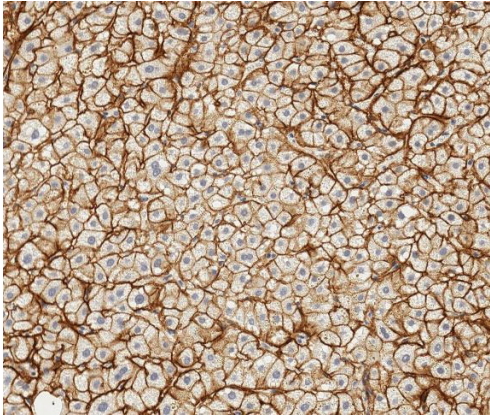
6
LC



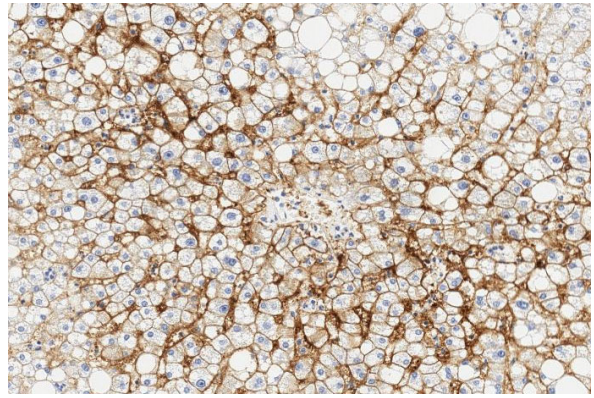
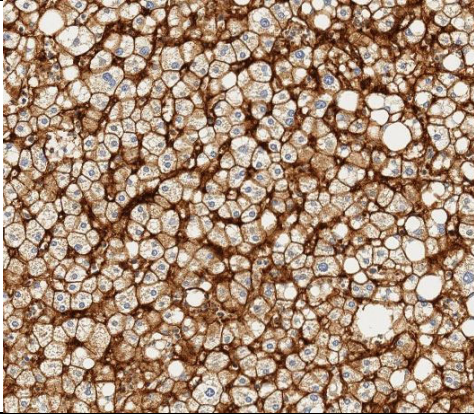
7



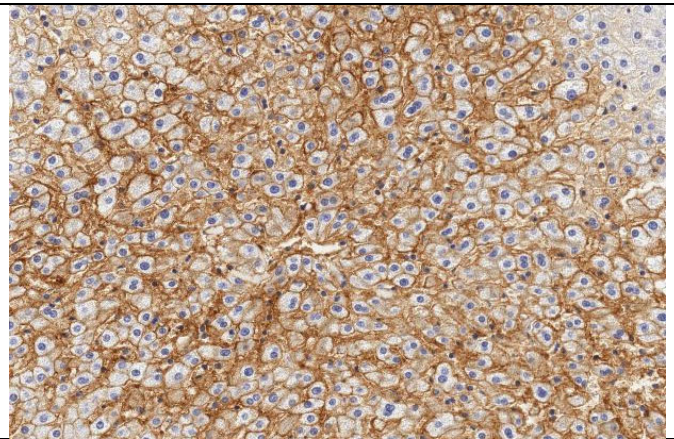
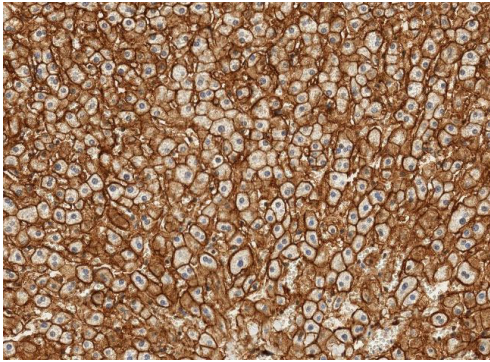
8



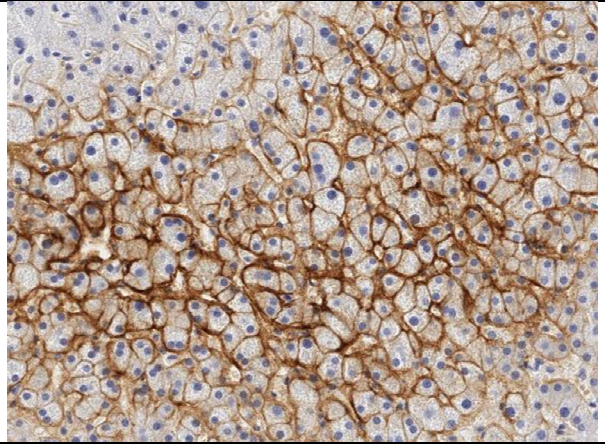
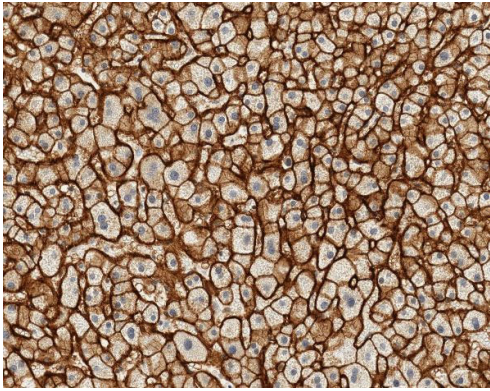
9
NM



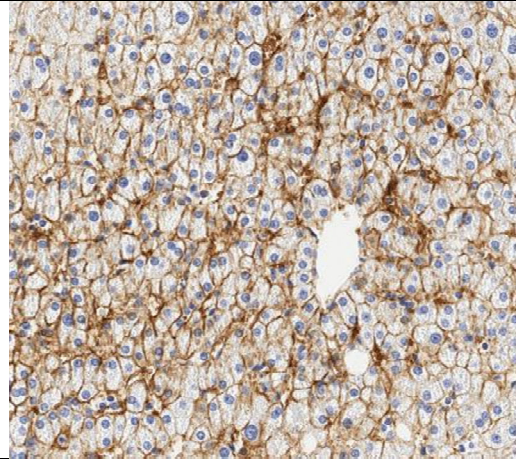
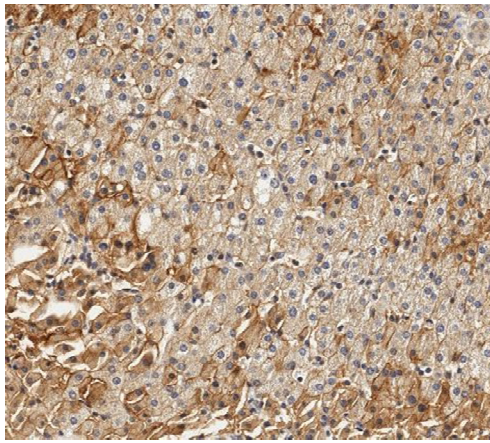
10
NM



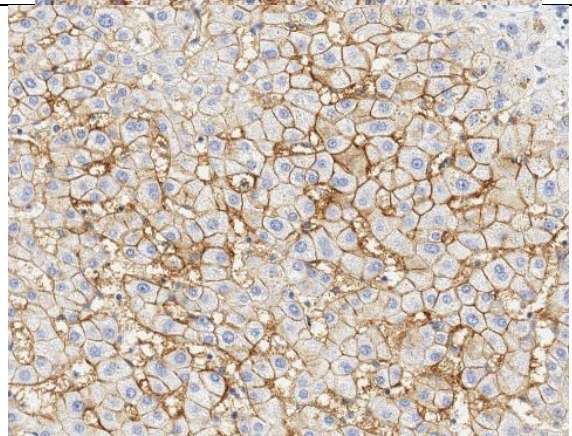
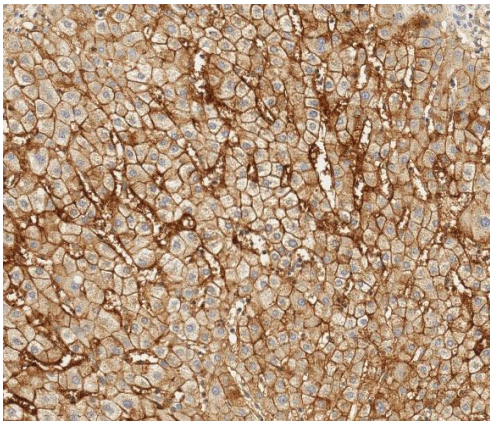
11

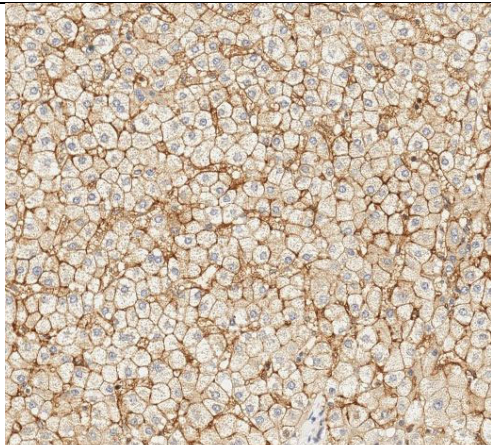
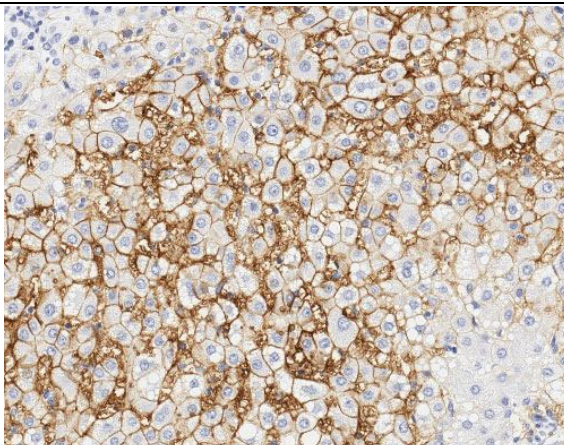
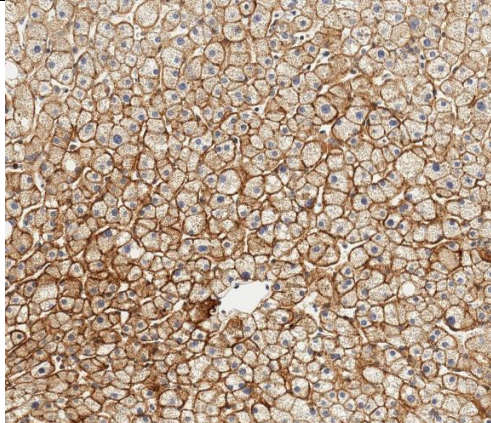
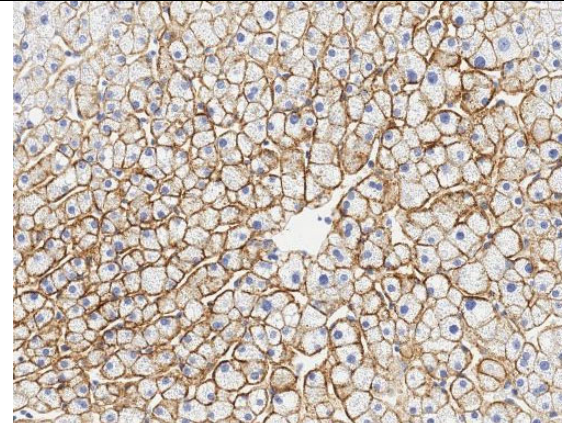
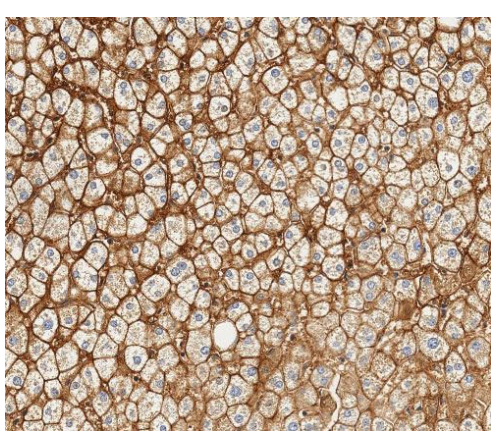
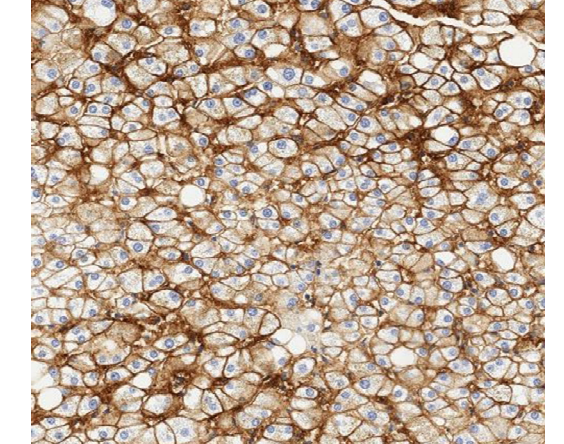


12

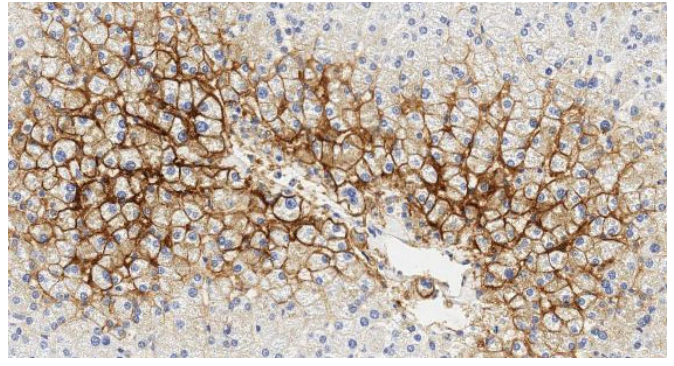
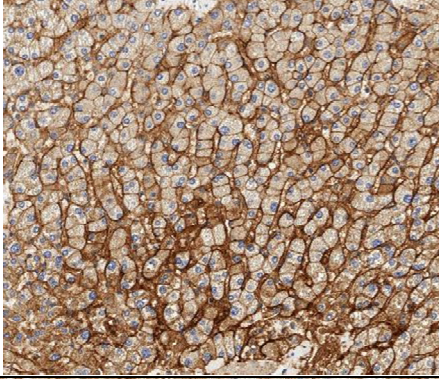


13
LC

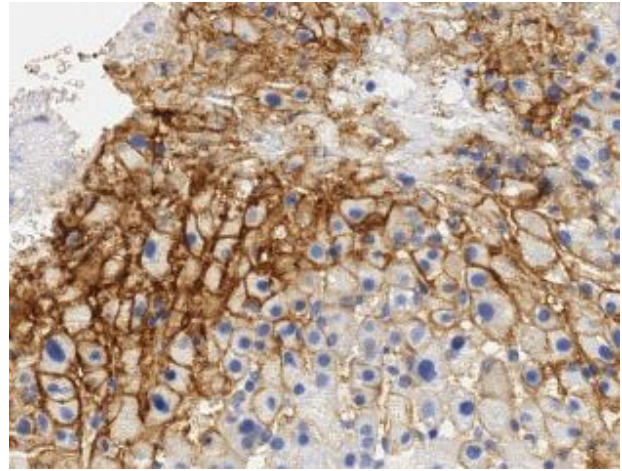
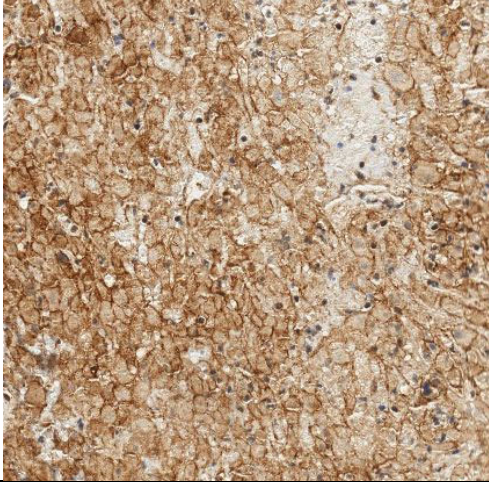


14 LC		
15		
16		

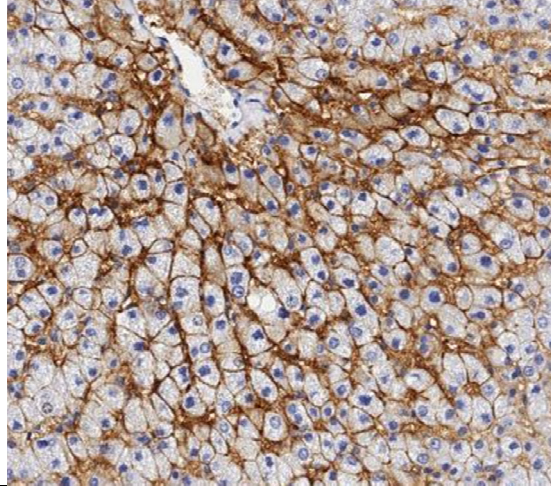
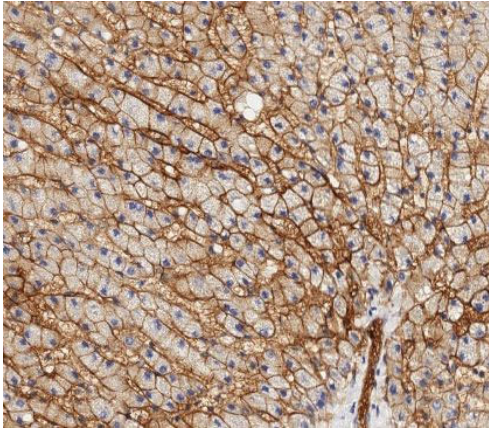
17



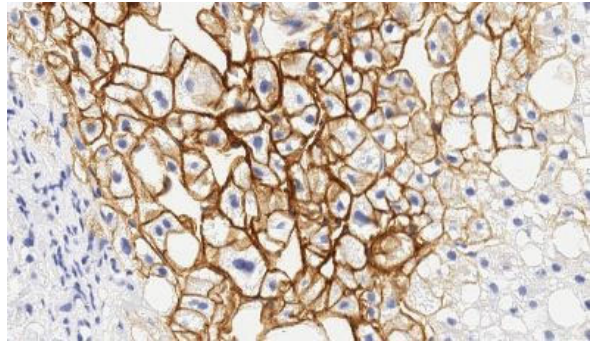
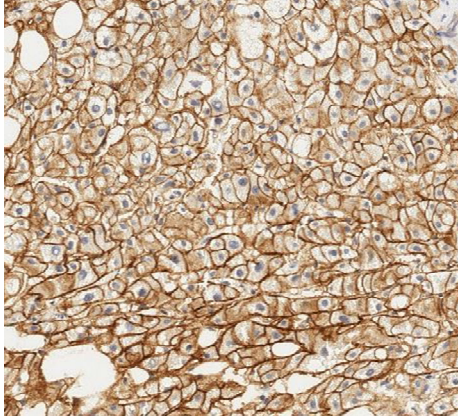
18



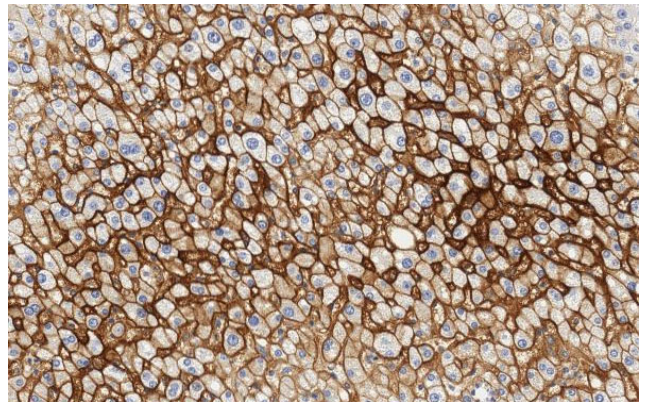
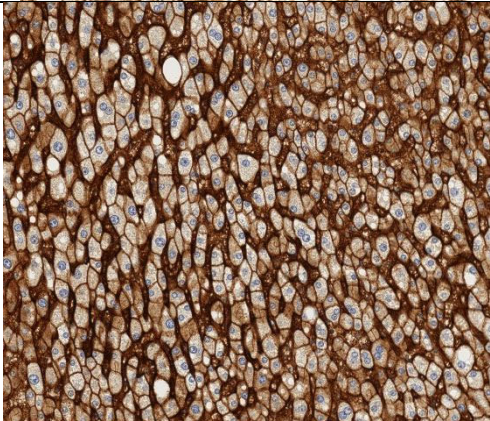
19



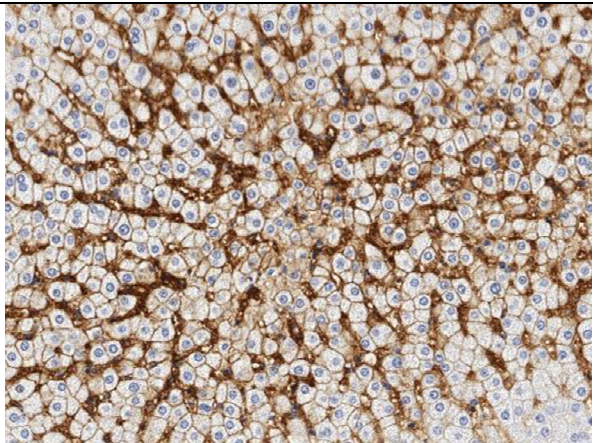
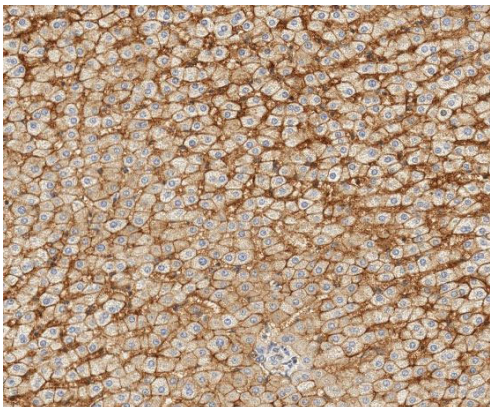
20
LC



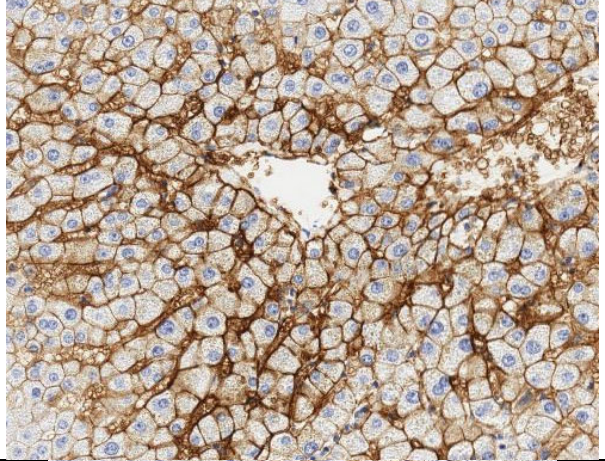
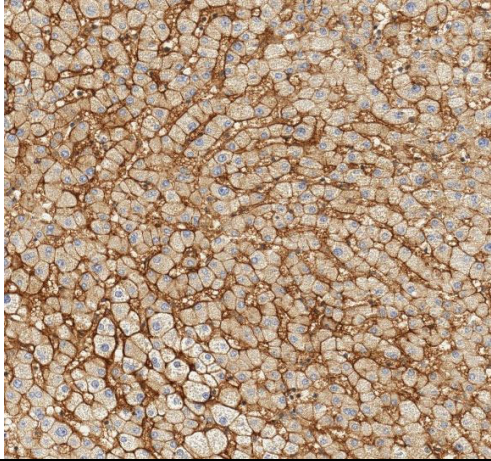
21



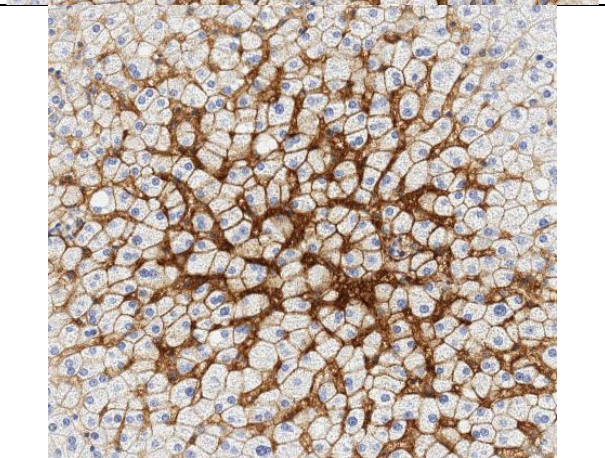
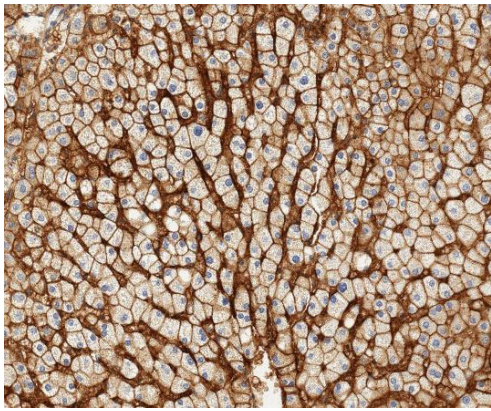
22
NM



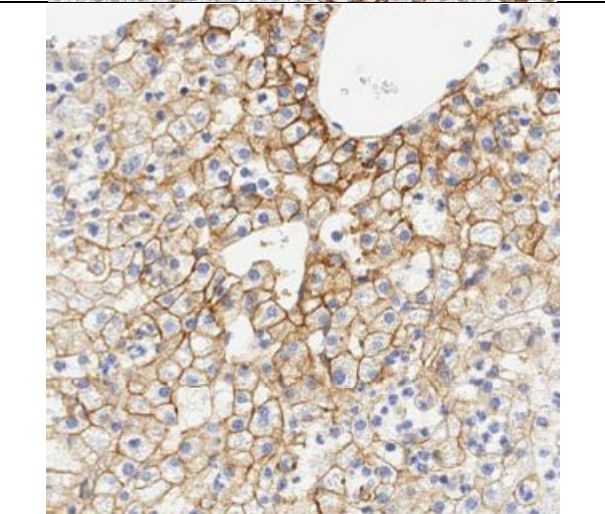
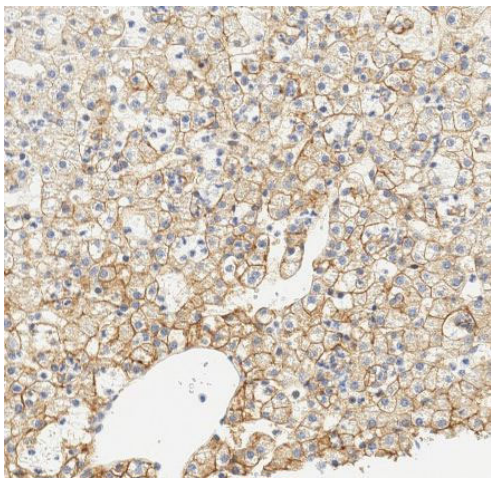
23



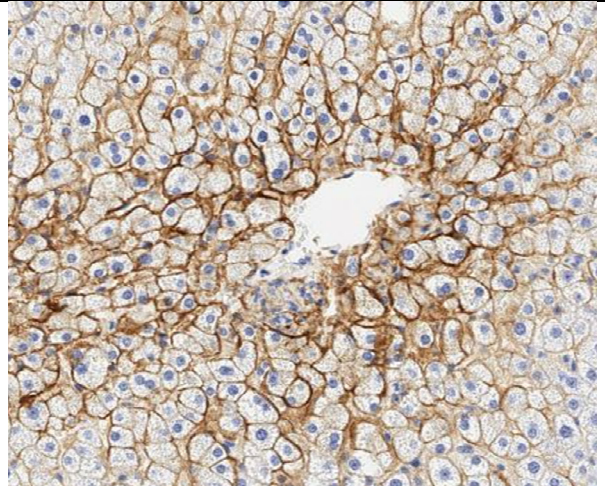
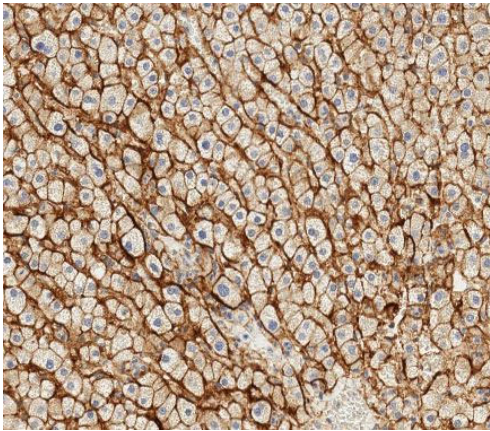
24



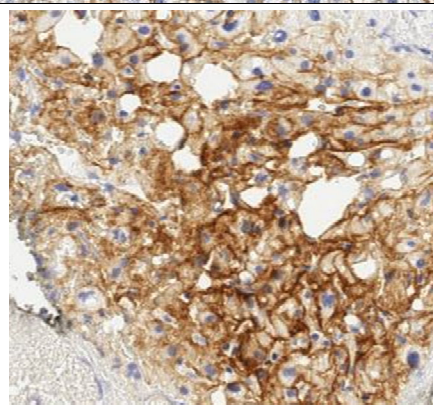
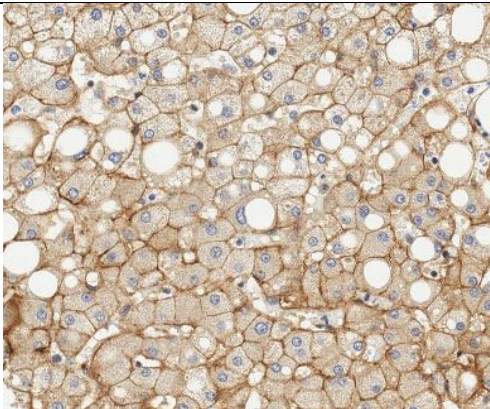
25



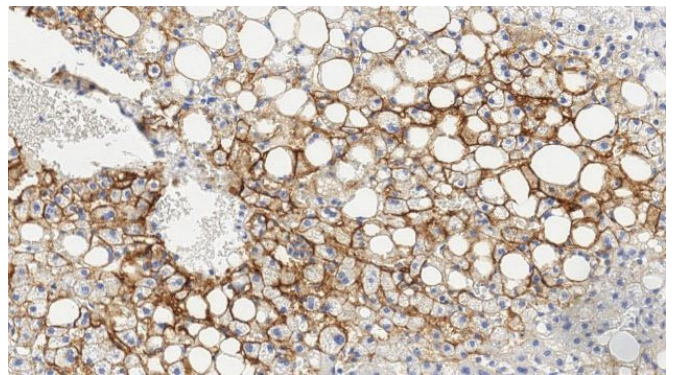
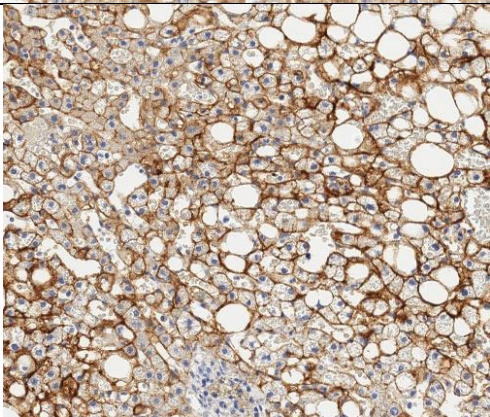
26

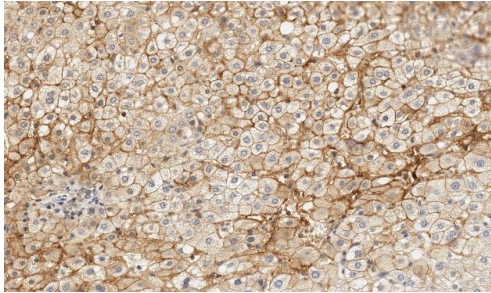
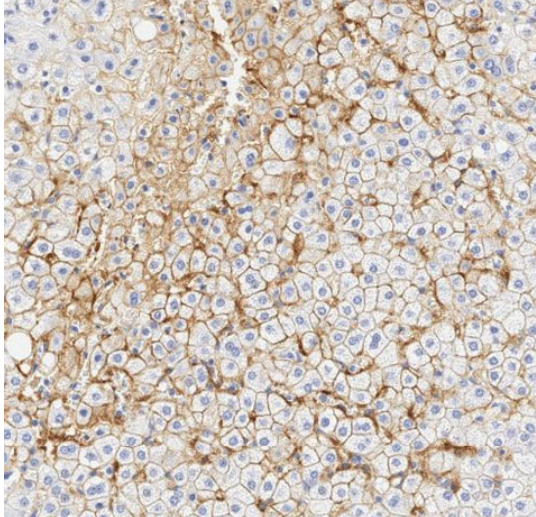
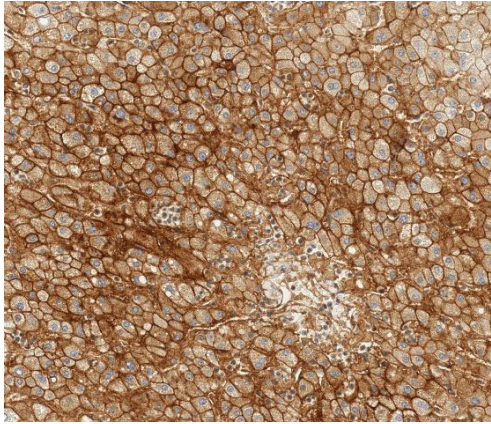
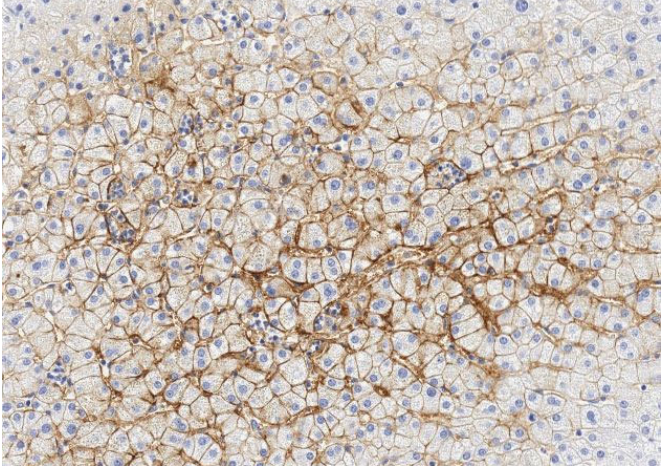
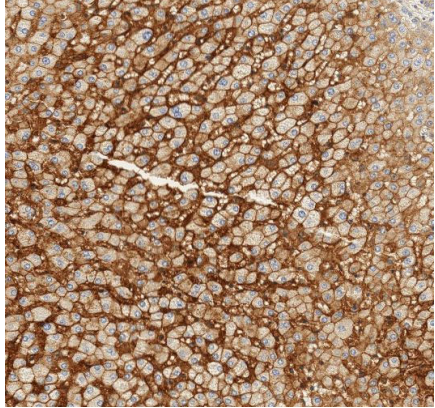
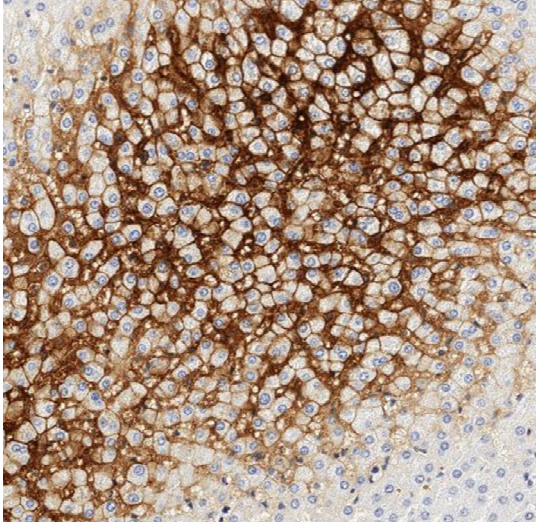


27

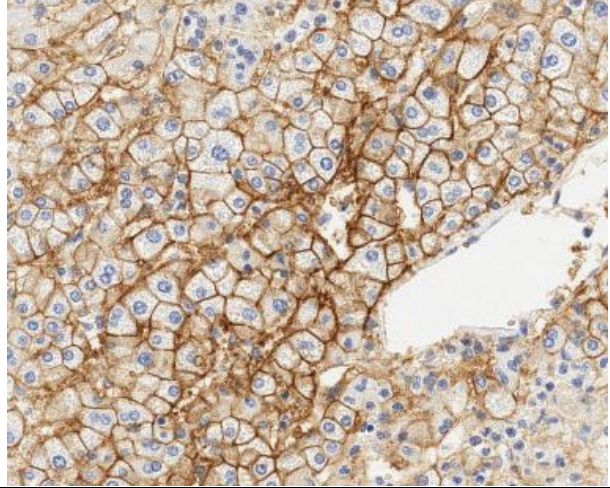
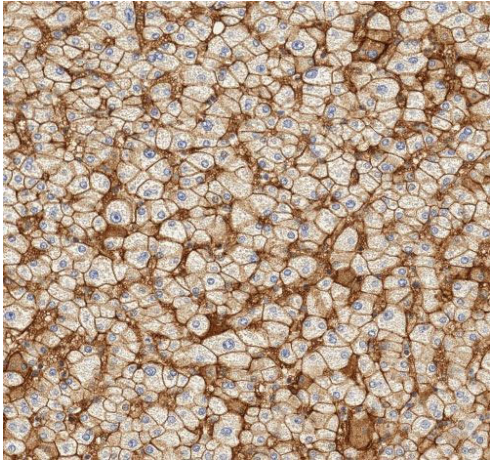


28

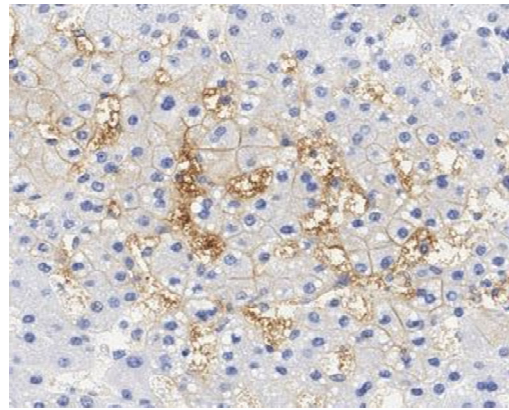
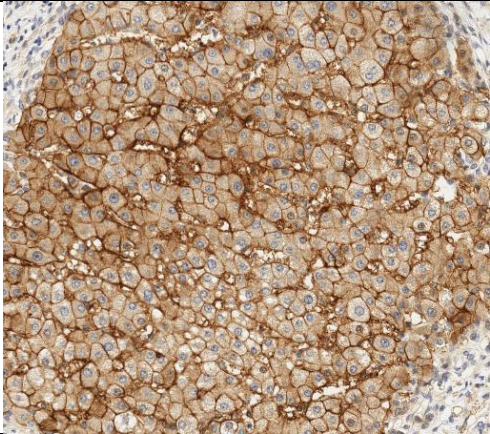


29		
30 NM		
31 NM		

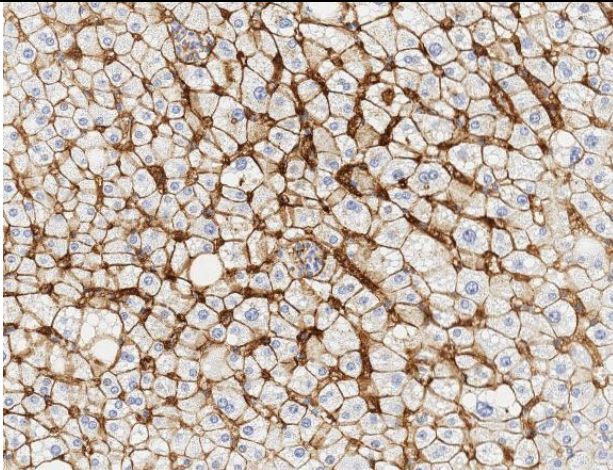
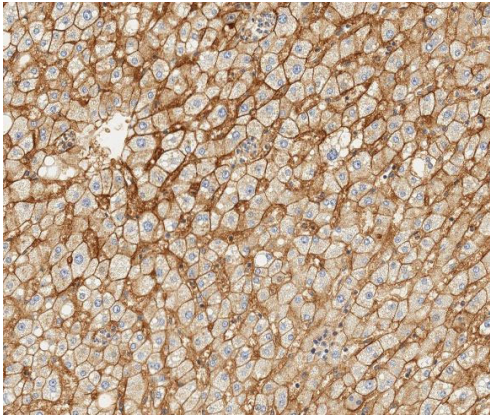
32



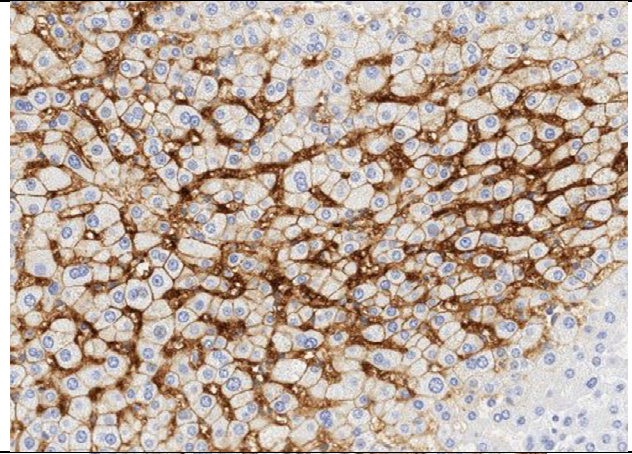
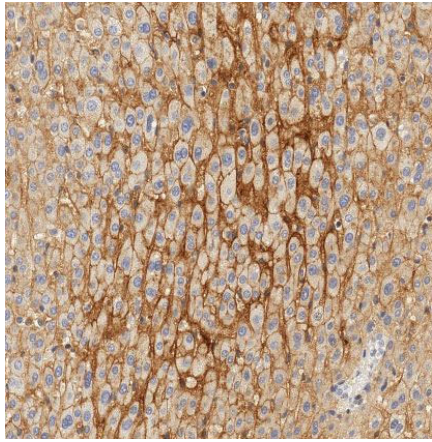
33
LC



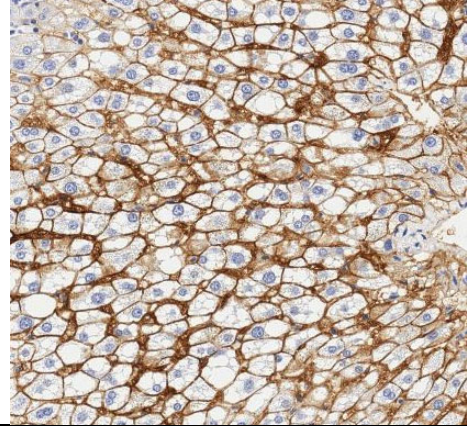
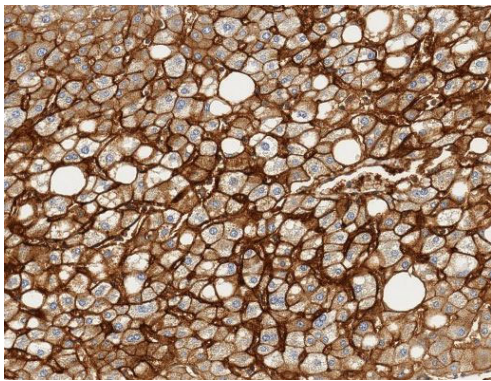
34
NM



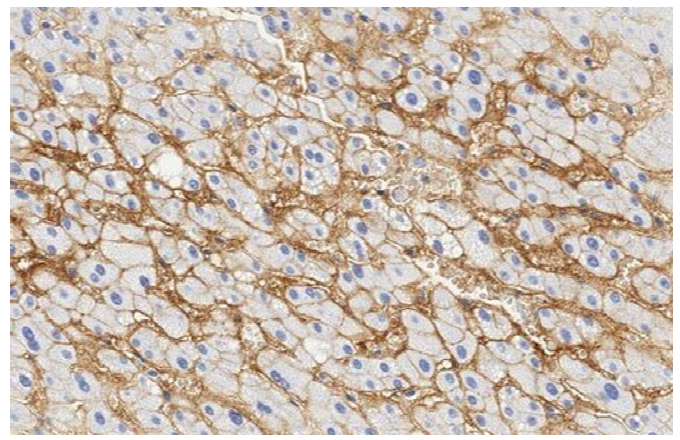
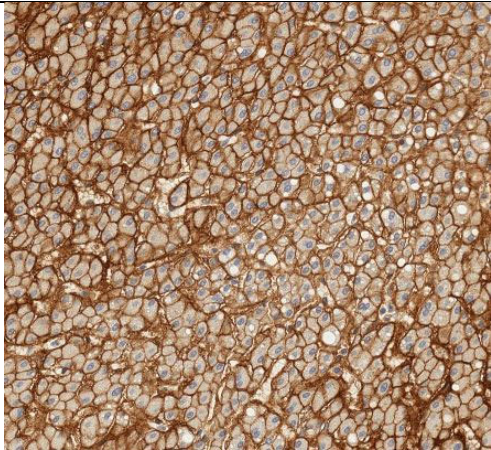
35



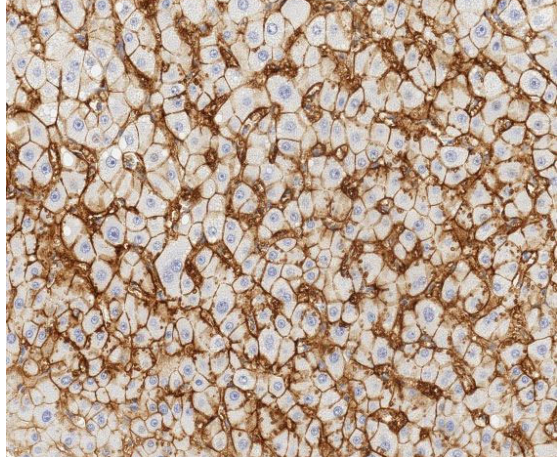
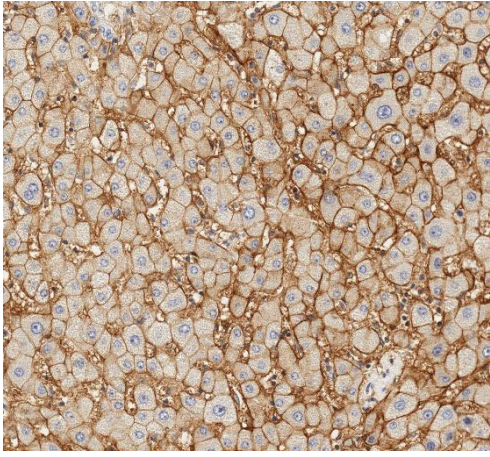
36



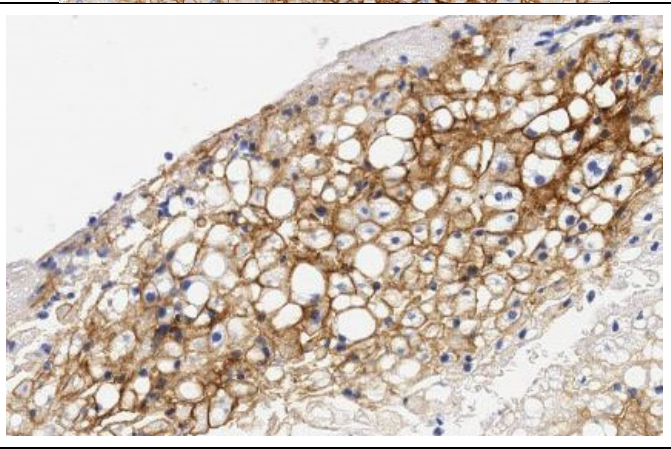
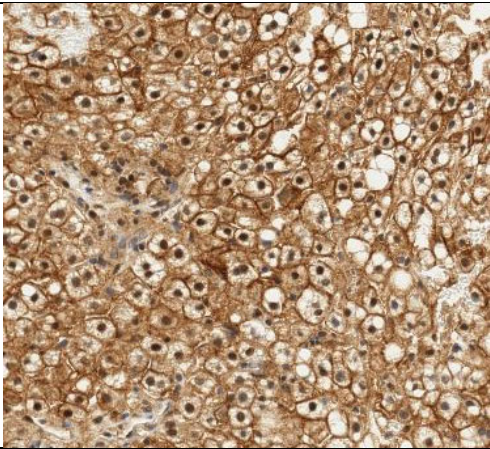
37
NM



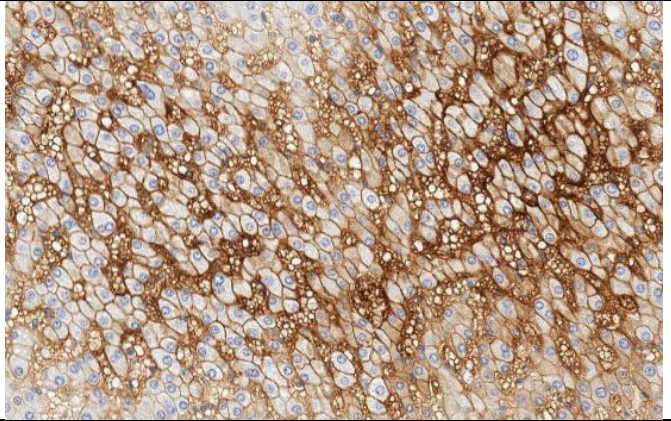
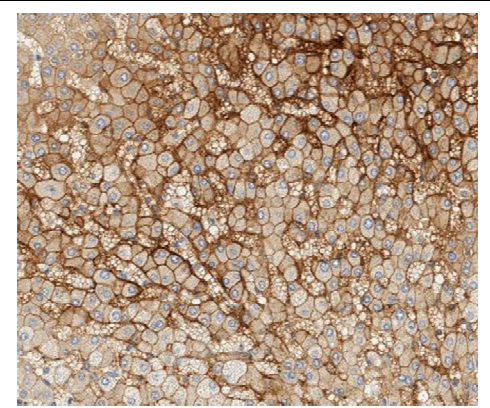
38
LC

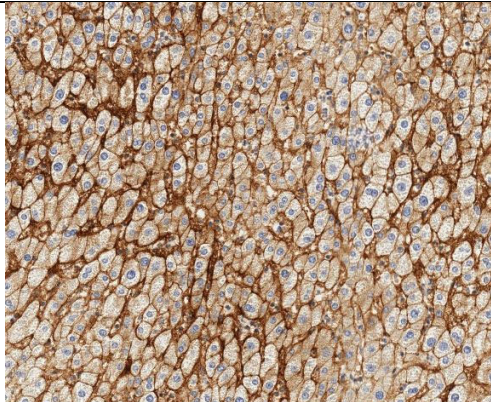
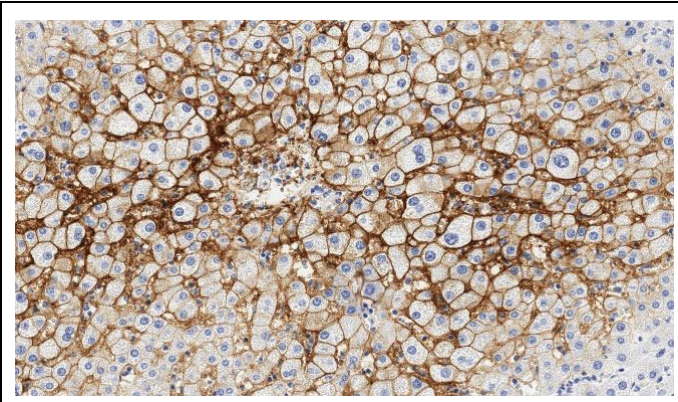
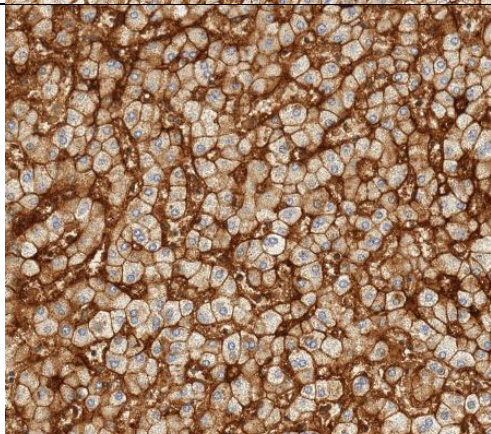
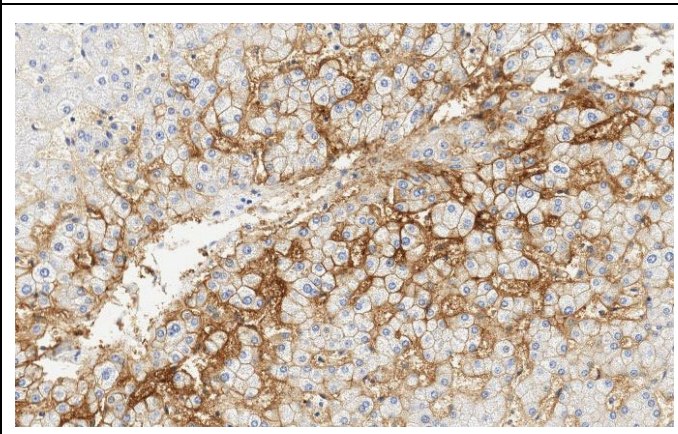
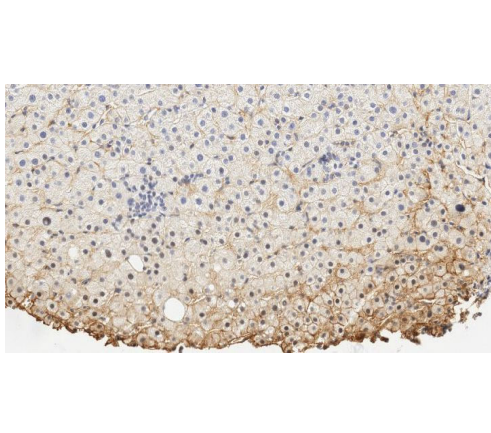
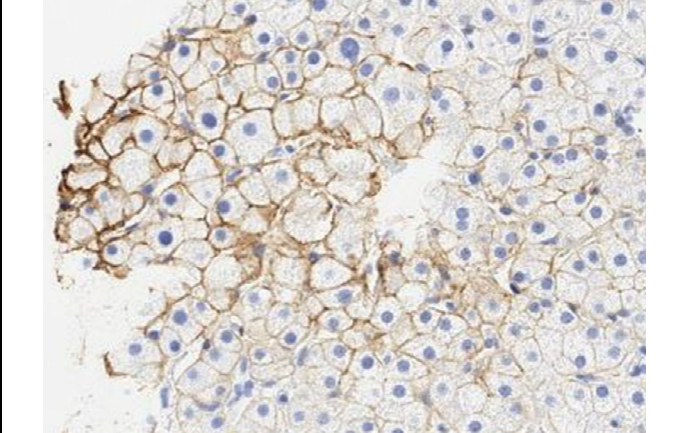


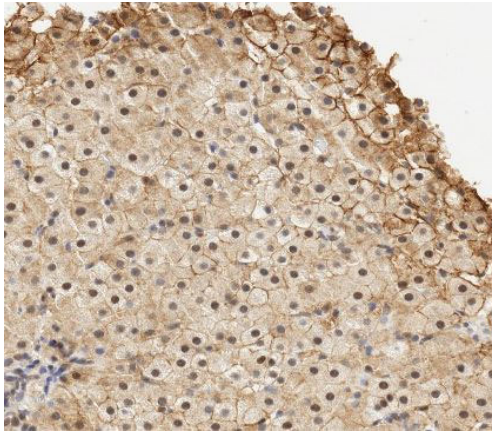
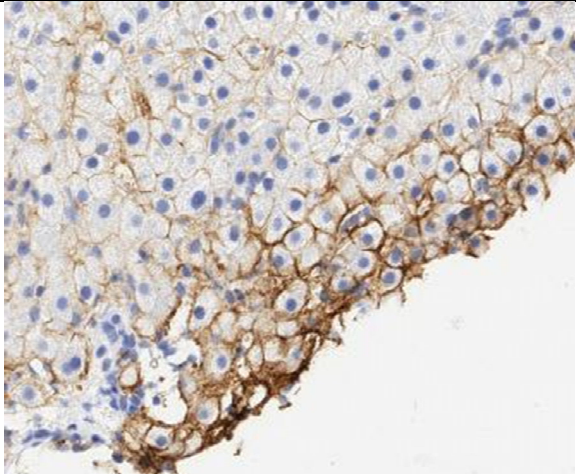
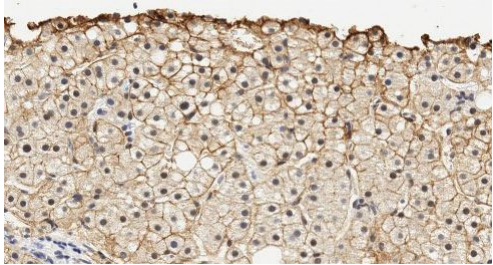
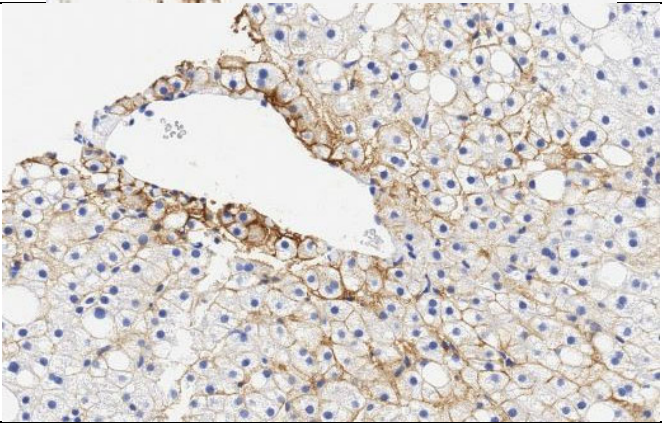
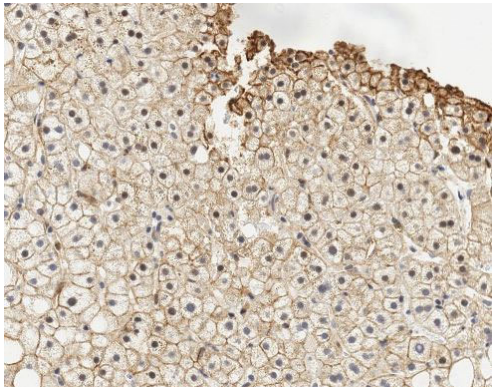
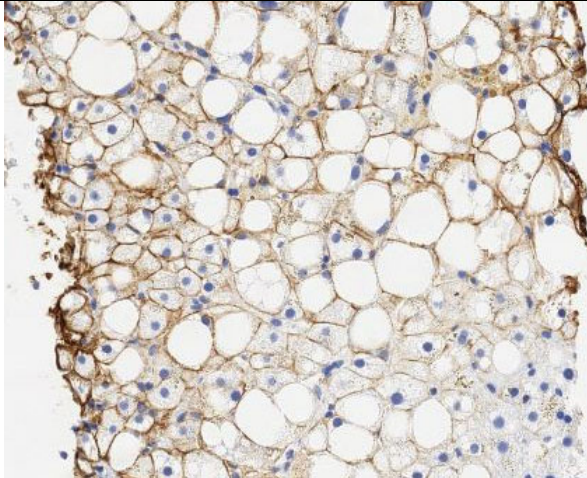
39



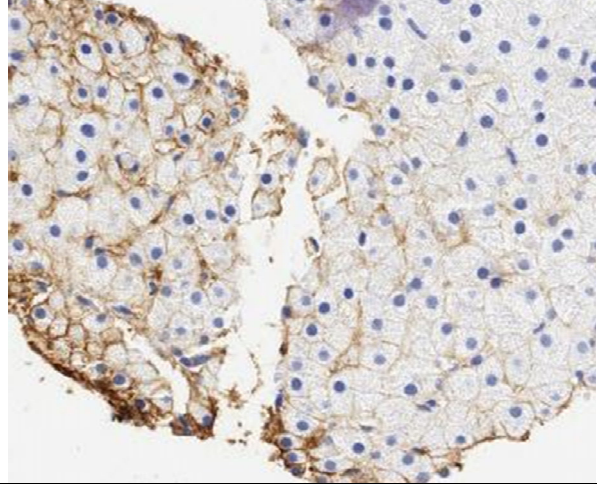
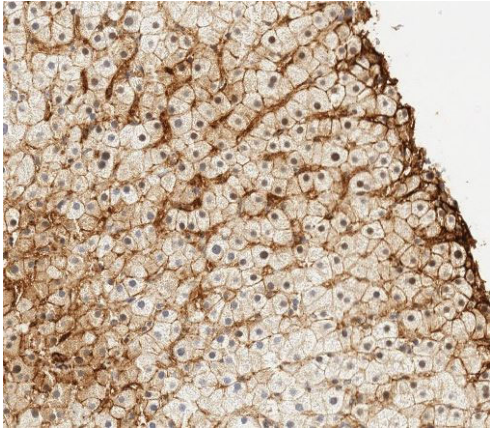
40



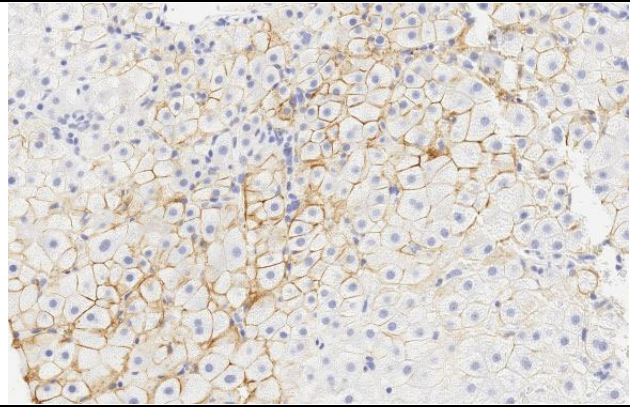
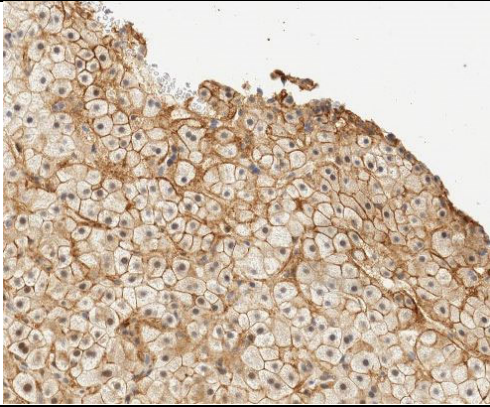
<p>41 CC</p>		
<p>42</p>		
<p>43 HCV</p>		

<p>44 HCV</p>		
<p>45 HCV</p>		
<p>46 HCV</p>		

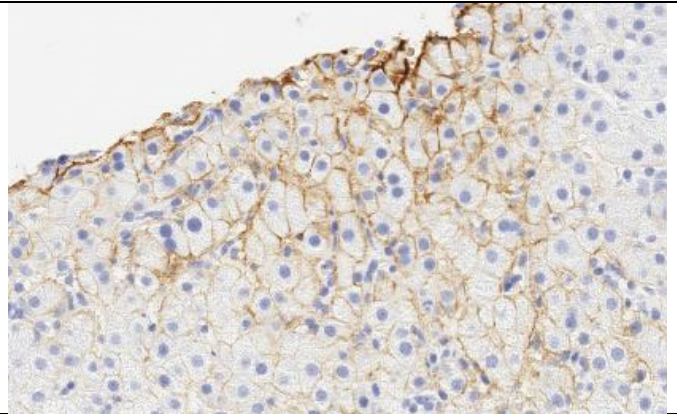
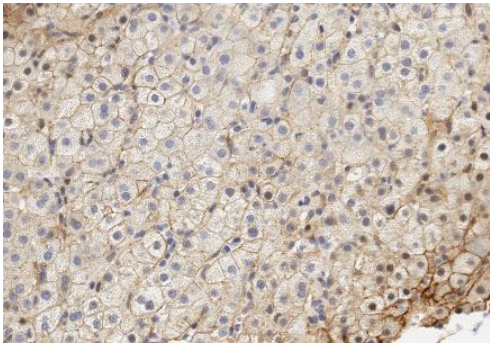
47
HCV



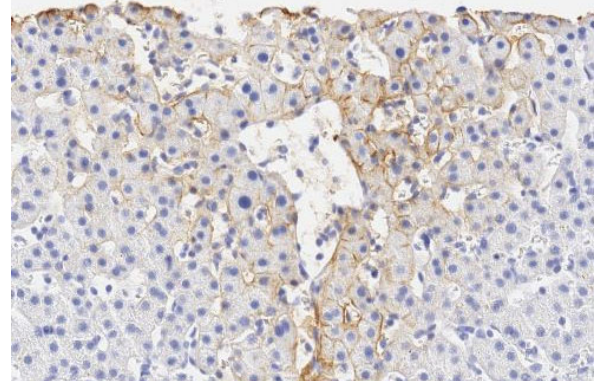
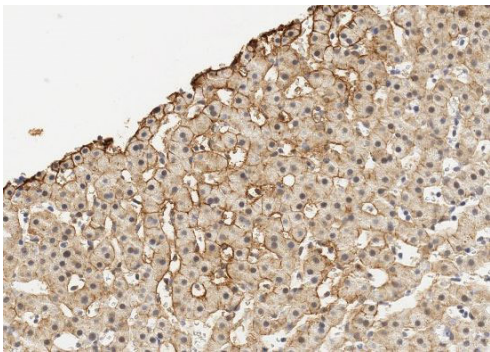
48
HCV



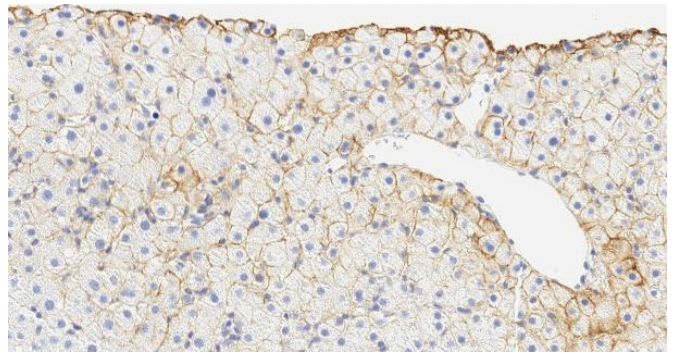
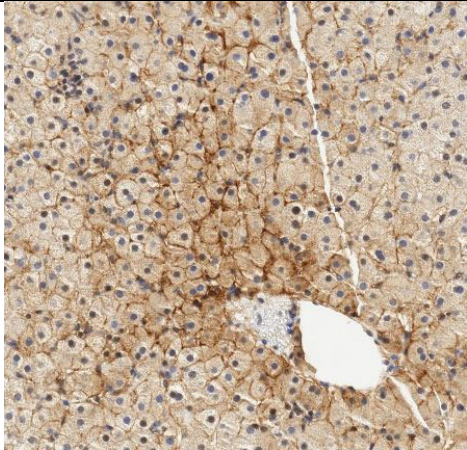
49
HCV



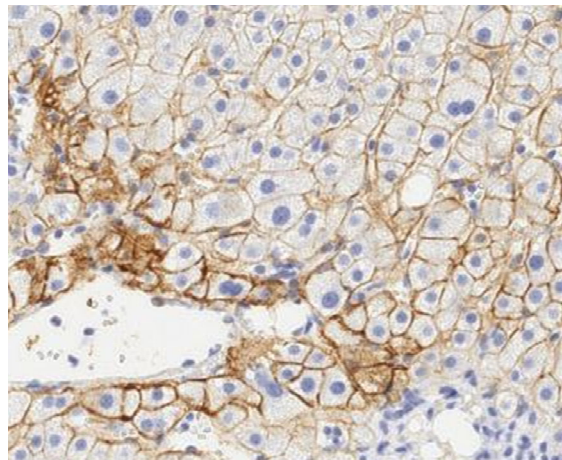
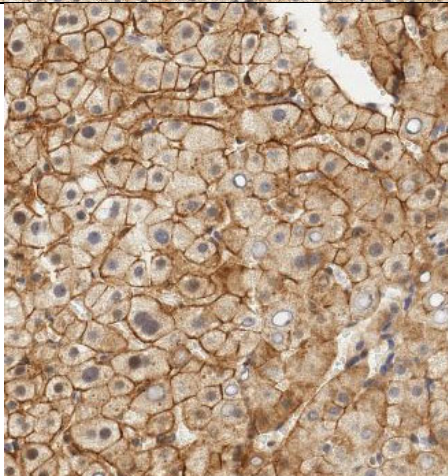
50
HCV



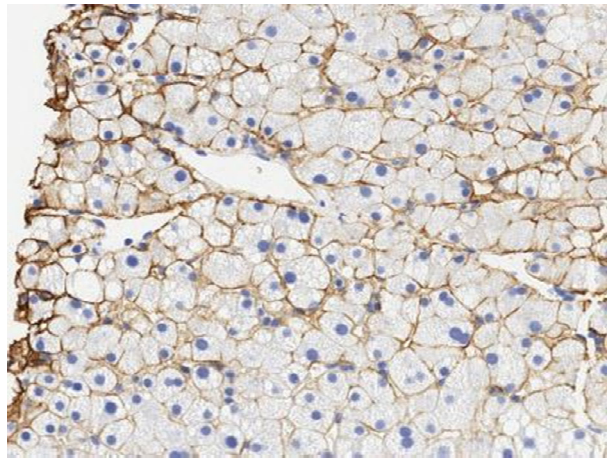
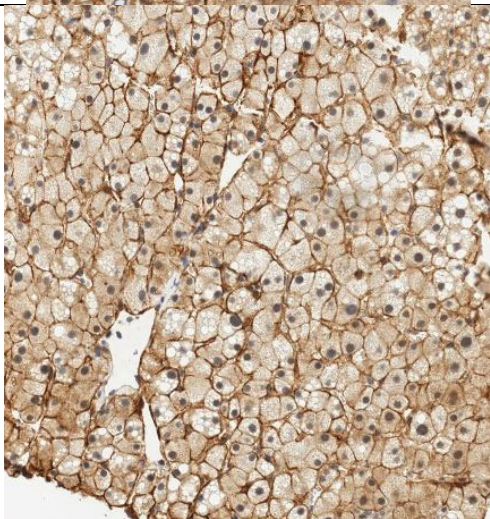
51
HCV

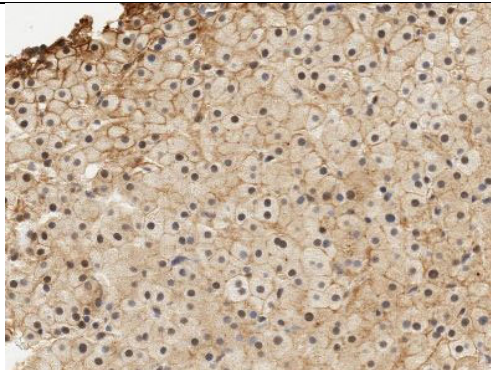
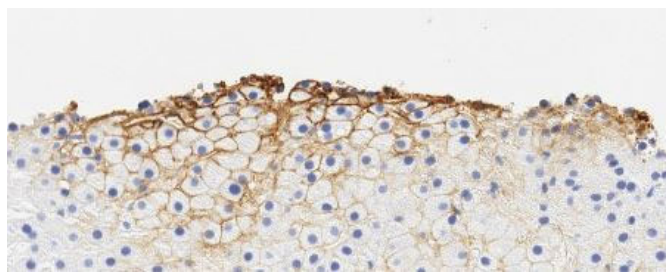
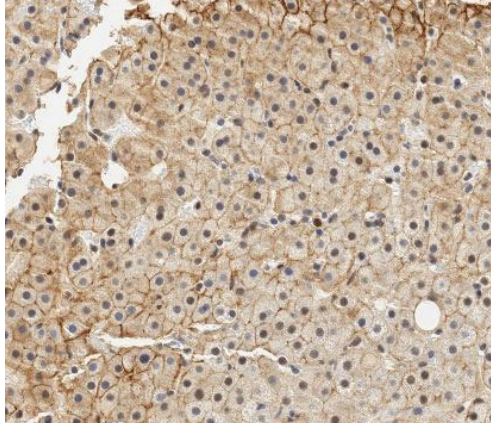
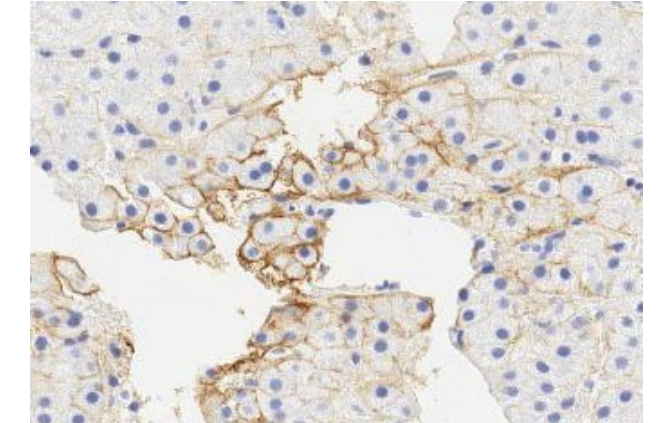
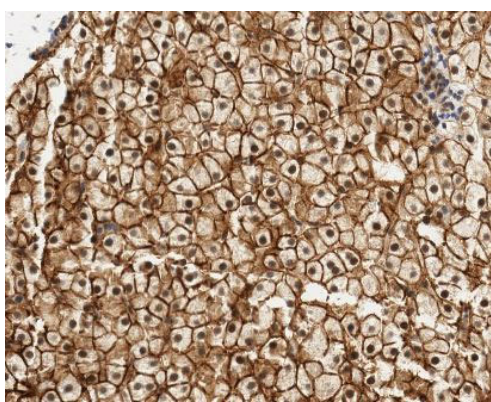
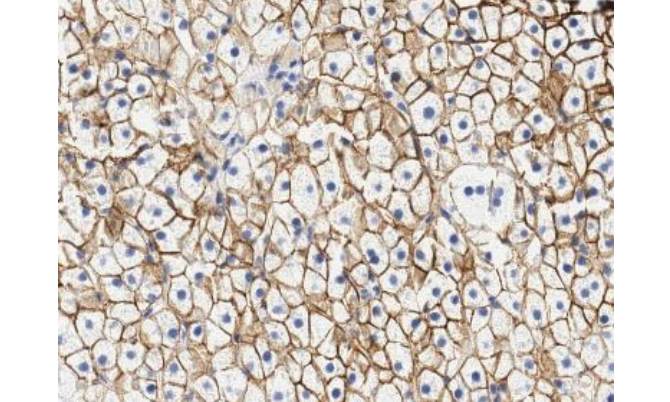
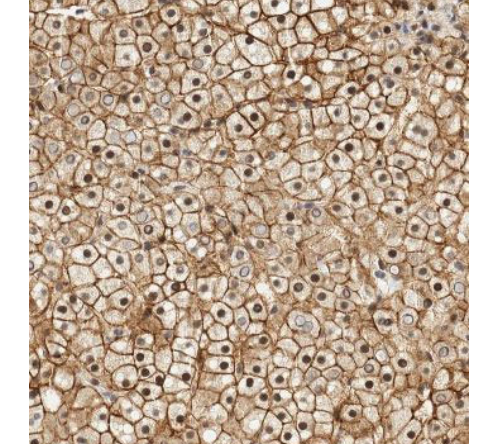
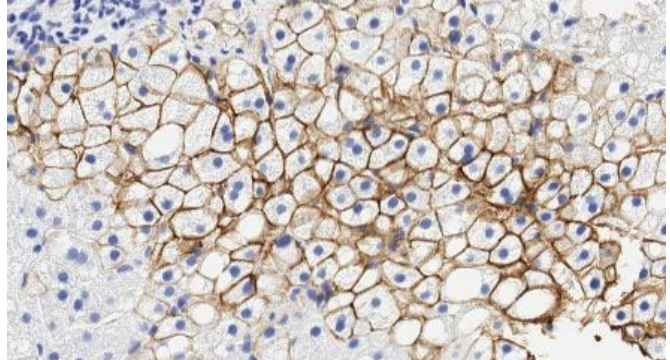


52
HCV

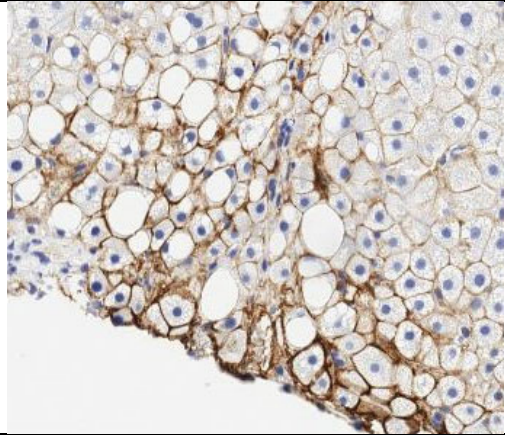
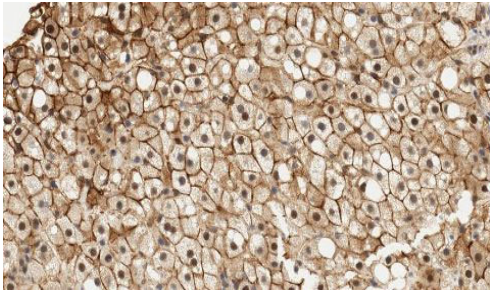


53
HCV

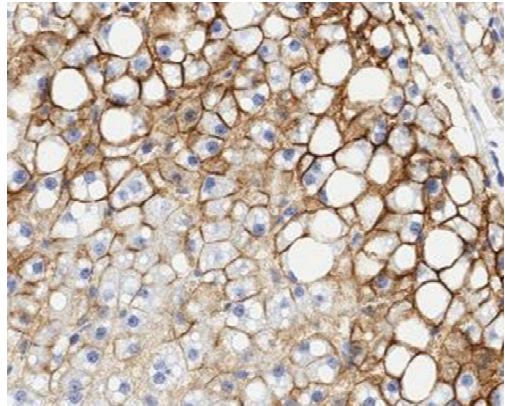
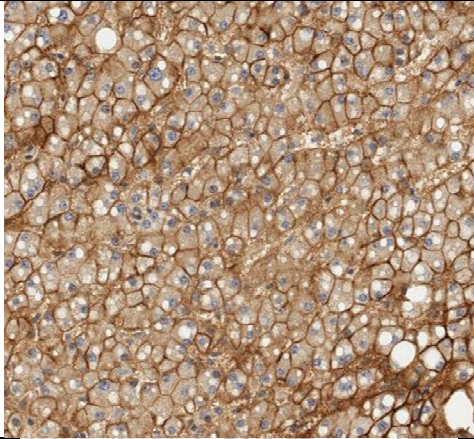


<p>54 HCV</p>		
<p>55 HCV</p>		
<p>56</p>		
<p>57</p>		

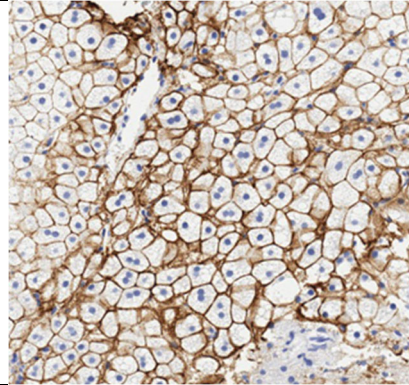
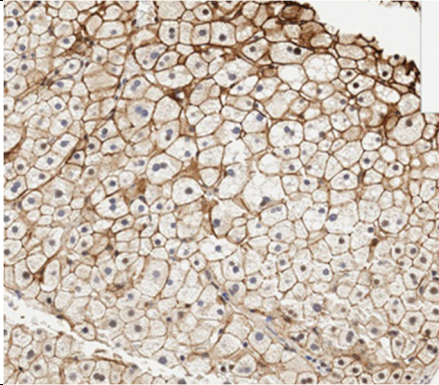
58
CC



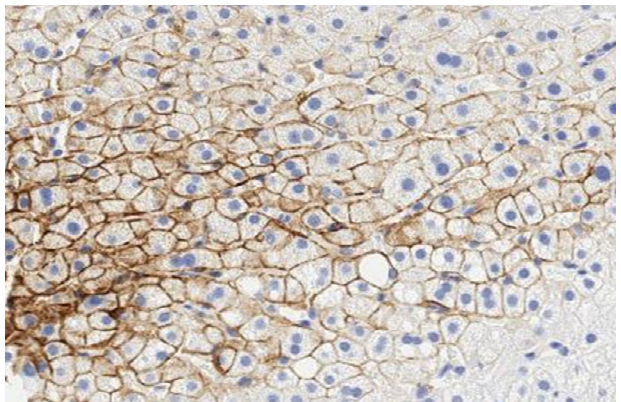
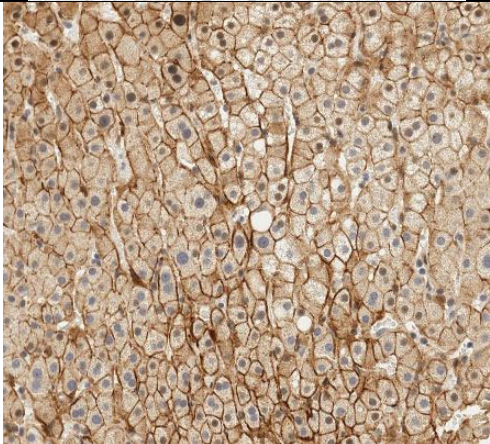
59

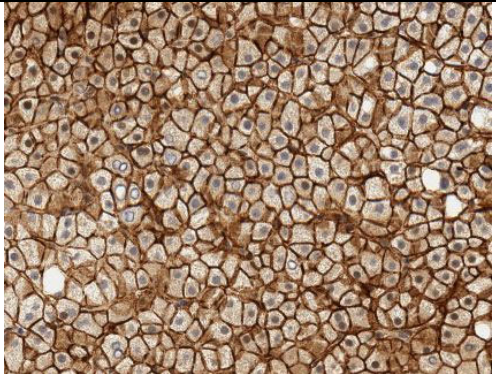
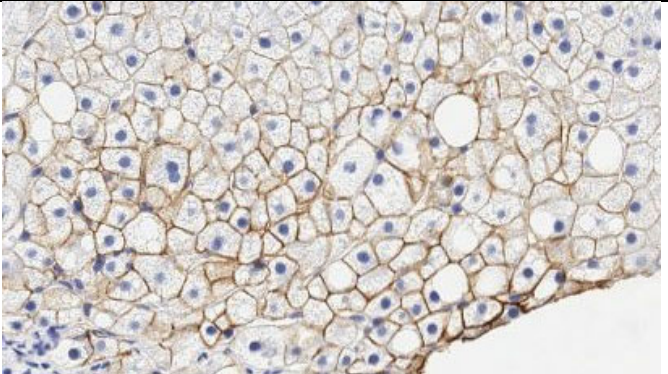
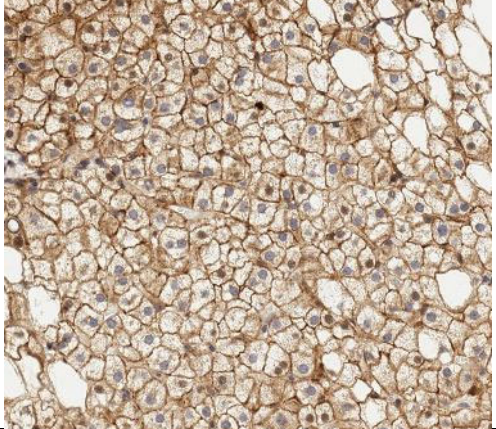
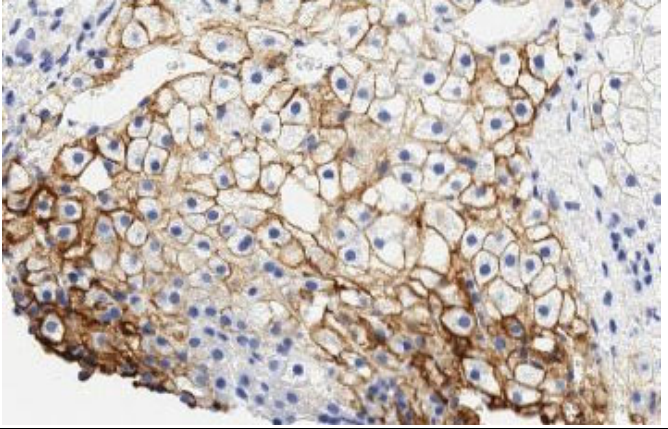
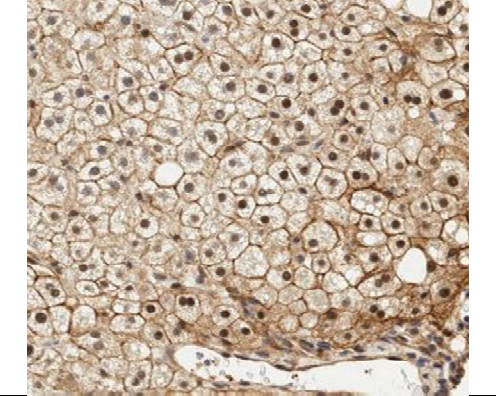
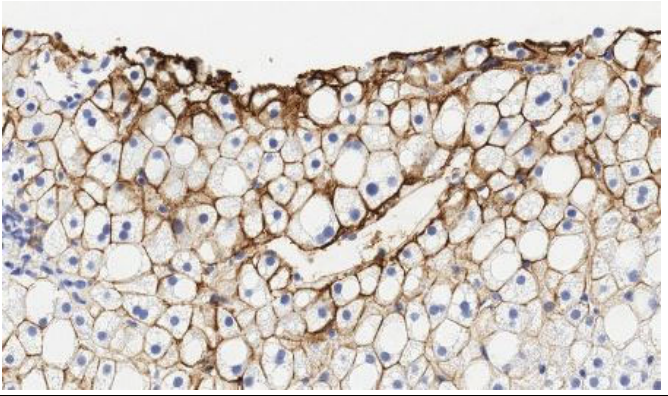
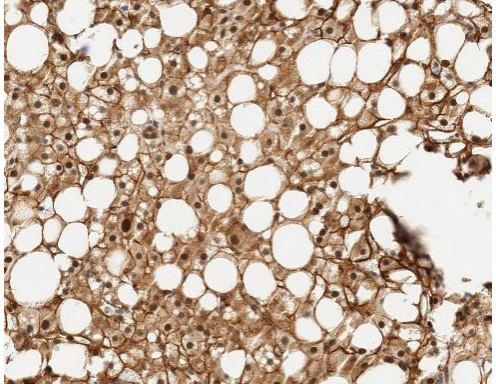
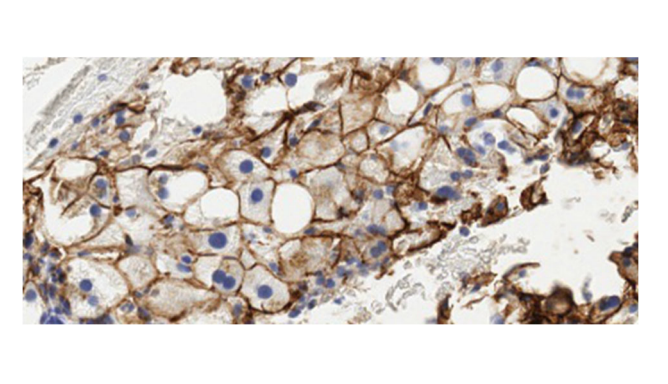


60

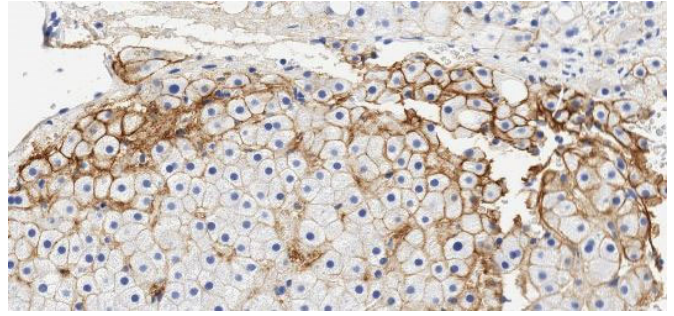
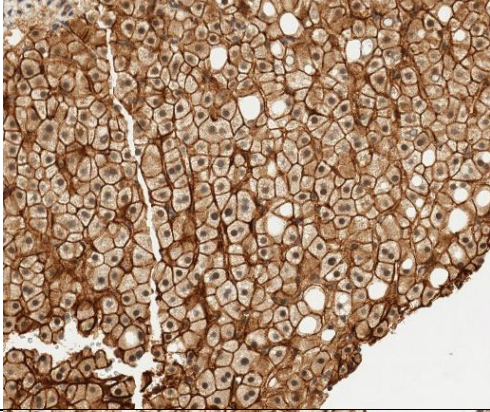


61

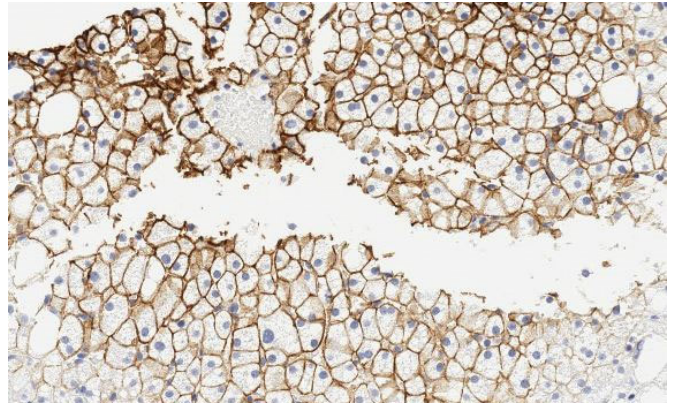
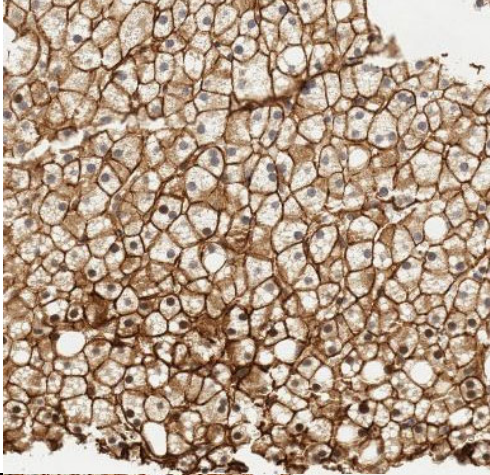


62		
63		
64		
65		

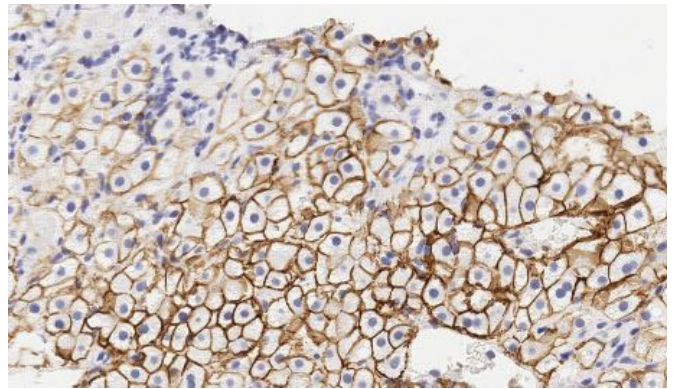
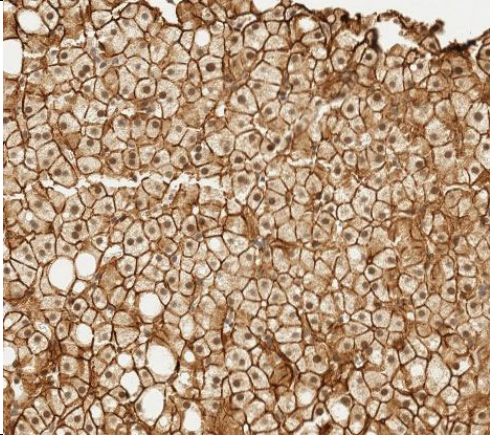
66



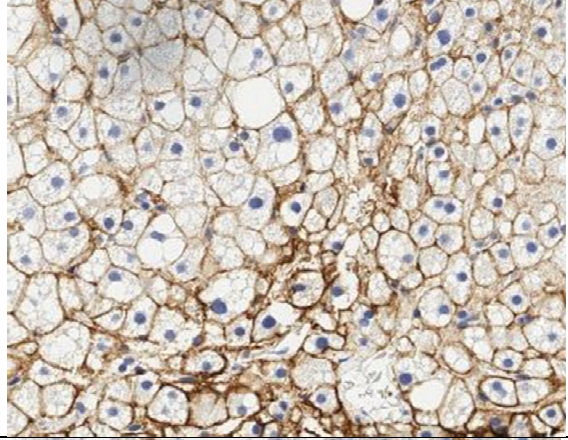
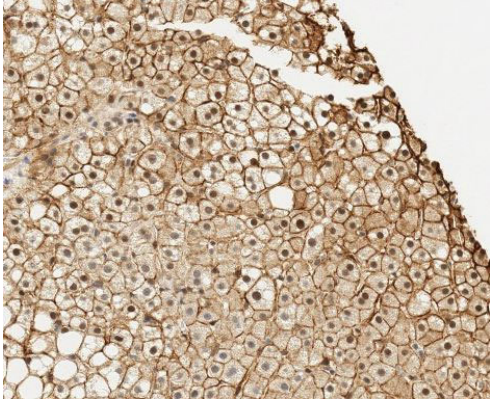
67



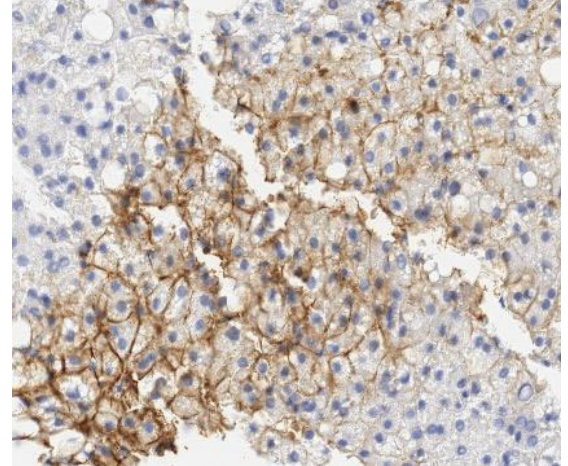
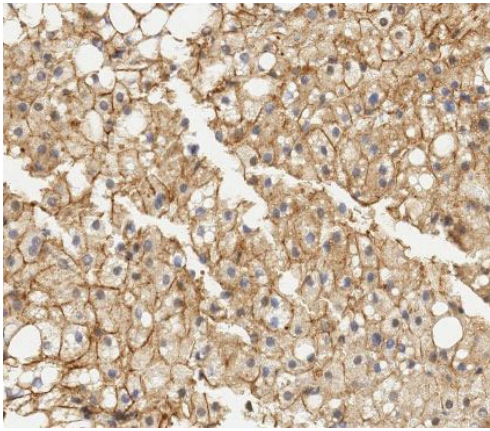
68



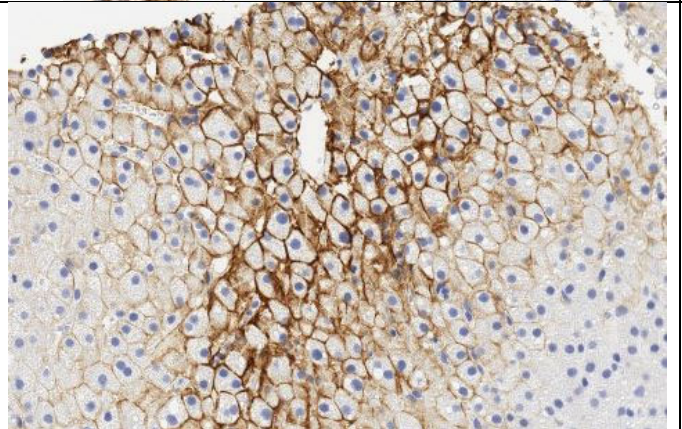
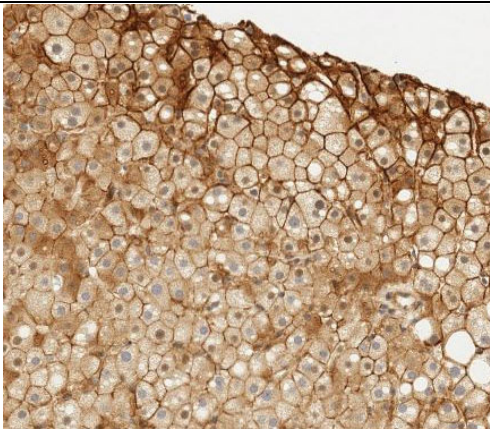
69

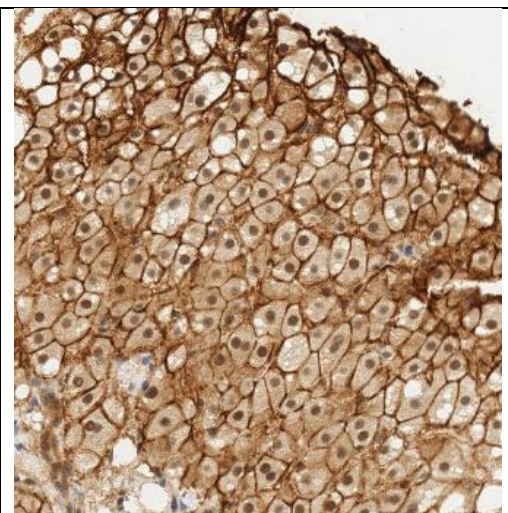
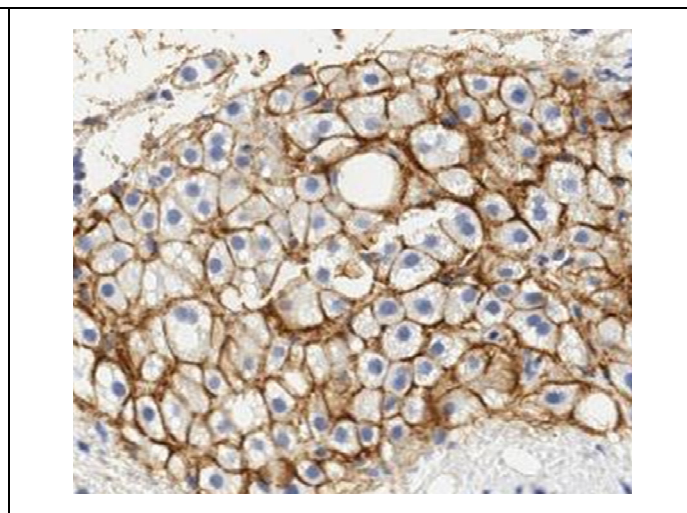
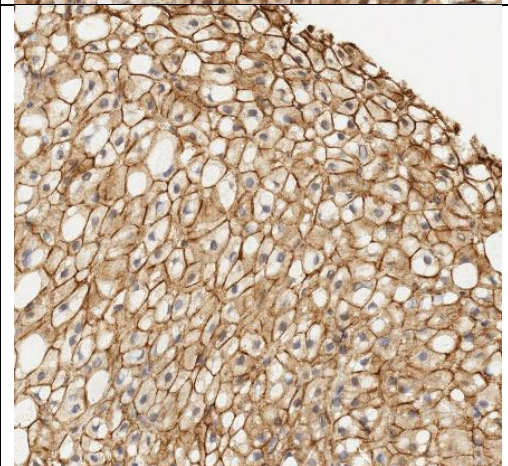
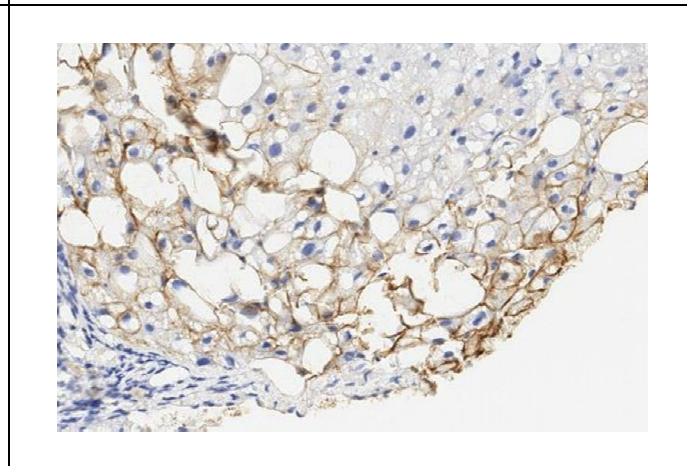
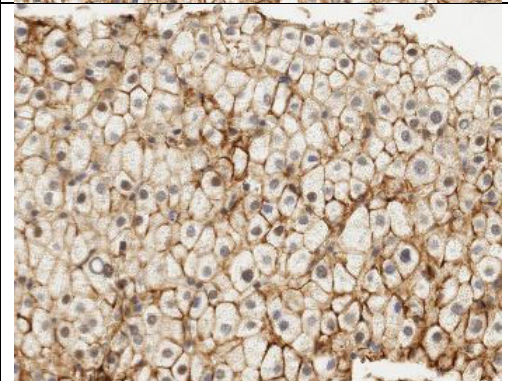
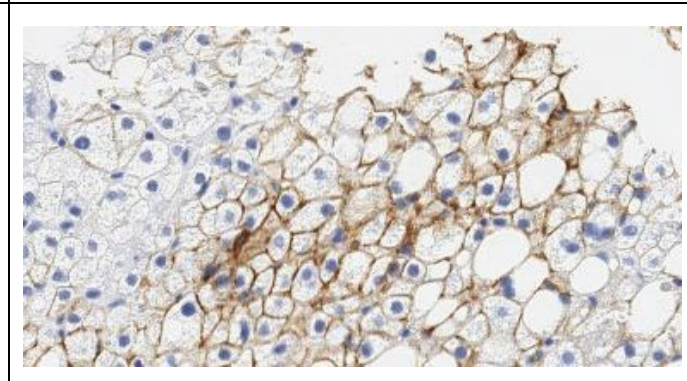
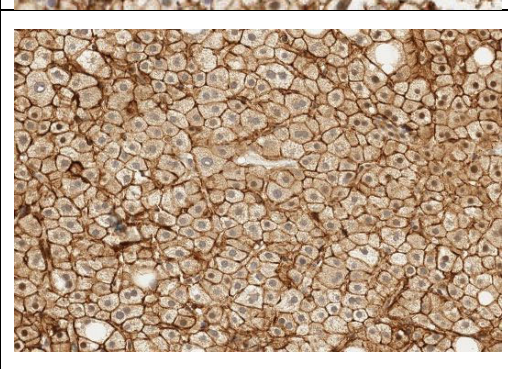
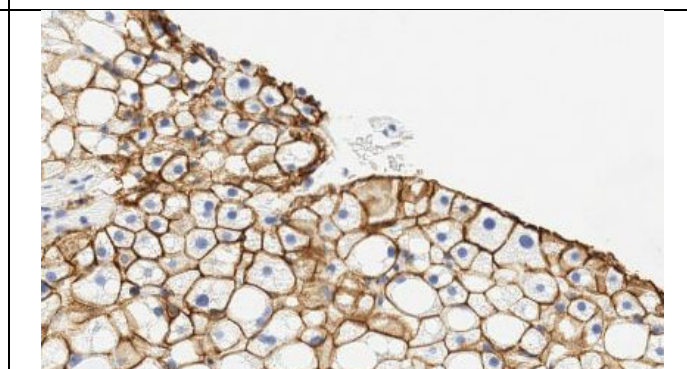


70

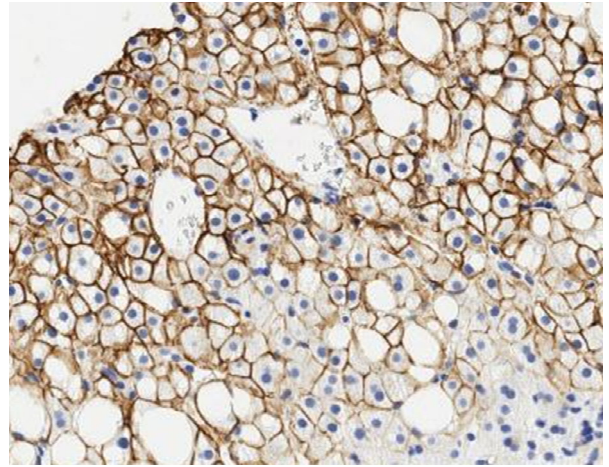
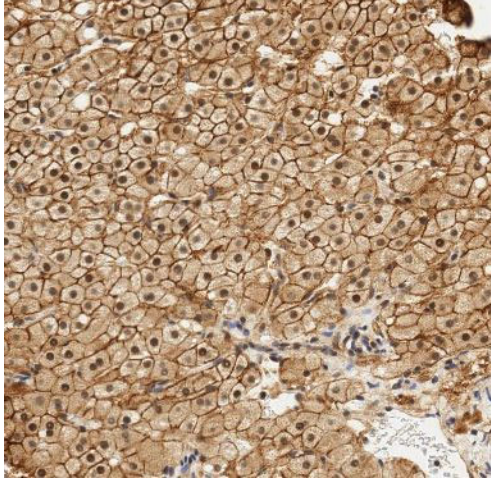


71

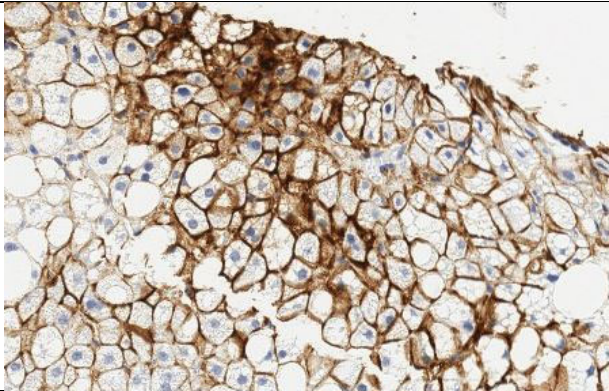
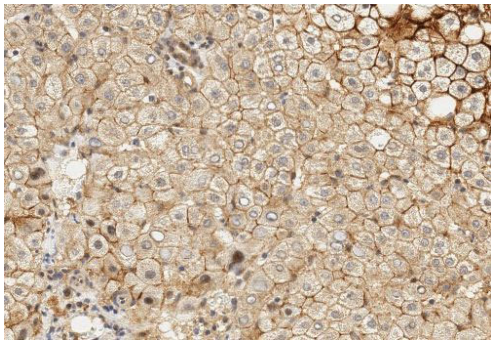


72		
73		
74		
75		

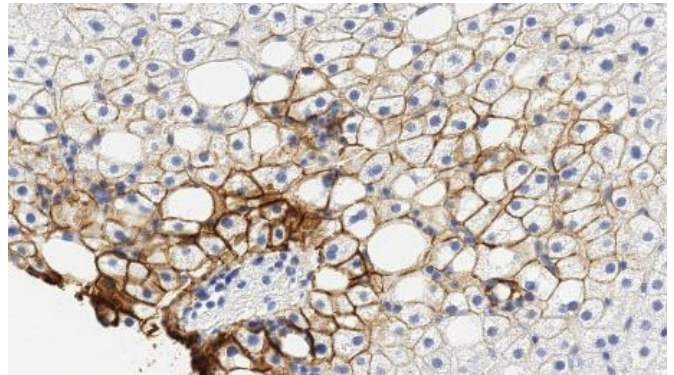
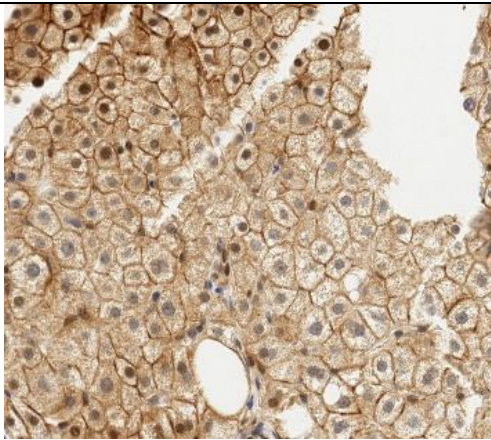
76



77



78



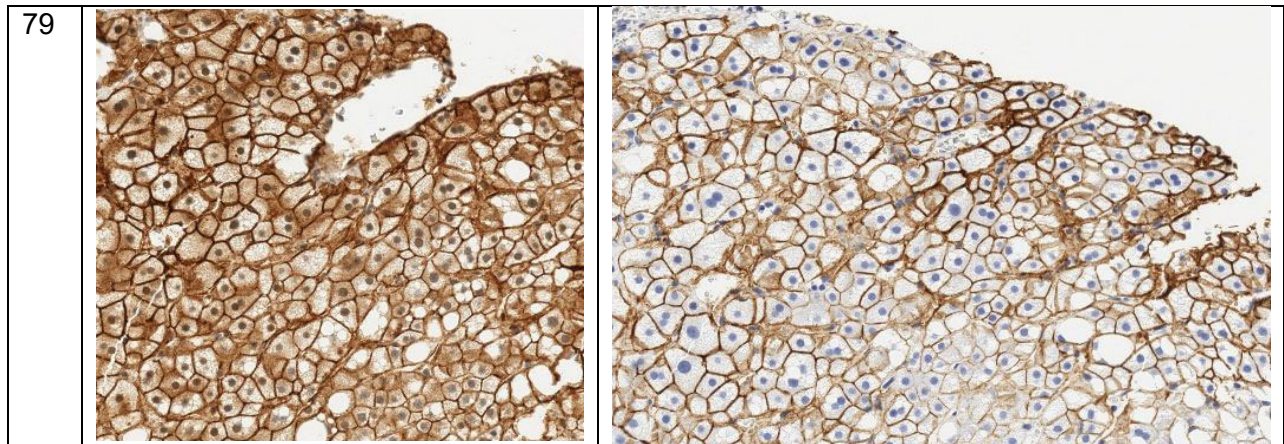


Fig. S X. IHC of OATP1B1 and OATP1B3. IHC of OATP1B1 (left) and OATP1B3 (right) staining are shown for each donor (n=79). Six liver cirrhotic tissues were labeled as LC. Thirteen HCV positive liver tissues were labeled as HCV. Eight normal liver tissues were labeled as NM. The two OATP1B1 c. 521 CC tissues were labeled as CC.

Table S II Prediction of OATP1B1 transmembrane (TM) domains. TM domains of OATP1B1 was predicted by Phobius (1) (<https://www.ebi.ac.uk/Tools/pfa/phobius/>) and TMPred (2) (https://embnet.vital-it.ch/software/TMPRED_form.html). The dashed area represents the 4th transmembrane domain. I indicates inner and O indicates outer orientation. The higher the probability or score, the confident the prediction is.

Helix #	Phobius (Kall et al., 2004)				TMPred (Hofmann et al., 1993)			
	Begin - End	Orientation	Length	Probability	Begin - End	Orientation	Length	Score
1	28 - 48	I - O	21	0.9980	25 - 48	I - O	24	1382
2	68 - 89	O - I	22	0.9900	65 - 88	O - I	24	1312
3	96 - 117	I - O	22	0.9998	96 - 121	I - O	26	2314
4	170 - 195	O - I	26	0.7984	169 - 196	O - I	28	607
5	207 - 230	I - O	24	0.9998	207 - 230	I - O	24	1861
6	258 - 279	O - I	22	0.9998	259 - 279	O - I	21	2142
7	337 - 356	I - O	20	0.9999	332 - 356	I - O	25	1899
8	376 - 395	O - I	20	1.0000	376 - 397	O - I	22	2402
9	407 - 428	I - O	22	0.9999	410 - 430	I - O	21	1792
10	534 - 560	O - I	27	0.9999	536 - 560	O - I	25	1491
11	572 - 595	I - O	24	0.9989	570 - 595	I - O	26	1192
12	624 - 646	O - I	23	0.9999	624 - 647	O - I	24	2056

References

1. Kall L, Krogh A, Sonnhammer EL. A combined transmembrane topology and signal peptide prediction method. *J Mol Biol.* 2004;338(5):1027-1036.
2. Hofmann K, Stoffel W. TMbase - A database of membrane spanning proteins segments. *Biol Chem Hoppe-Seyler.* 1993;374:166.